Manuscript prepared for Atmos. Chem. Phys. Discuss.
with version 2015/04/24 7.83 Copernicus papers of the LaTeX class copernicus.cls.
Date: 1 January 2016

Mixing layer height and ~~the~~ its implications for air pollution over Beijing, China

G. Tang[1], J. Zhang[2], X. Zhu[1], T. Song[1], C. Münkel[3], B. Hu[1], K. Schäfer[4], Z. Liu[1], L. Wang[1], J. Xin[1], P. Suppan[4], and Y. Wang[1]

[1]State Key Laboratory of Atmospheric Boundary Layer Physics and Atmospheric Chemistry (LAPC), Institute of Atmospheric Physics, Chinese Academy of Sciences, Beijing 100029, China
[2]Key Laboratory of Middle Atmosphere and Global Environment Observation (LAGEO), Institute of Atmospheric Physics, Chinese Academy of Sciences, Beijing 100029, China
[3]Vaisala GmbH, 22607 Hamburg, Germany
[4]Karlsruhe Institute of Technology (KIT), Institute of Meteorology and Climate Research, Atmospheric Environmental Research (IMK-IFU), 82467 Garmisch-Partenkirchen, Germany

Correspondence to: Y. Wang (wys@mail.iap.ac.cn)

Discussion Paper | Discussion Paper | Discussion Paper | Discussion Paper |

Abstract

The mixing layer is an important meteorological factor that affects ~~atmospheric pollution. A studyof atmospheric pollution in the Beijing area was performed~~ air pollution. In this study, the atmospheric mixing layer height (MLH) was observed in Beijing from July 2009 to December 2012 ~~,~~ using a ceilometer~~, to observe and study the atmospheric mixing layer height (MLH). Based on a comparison and validation of multiple types of~~ . By comparison with radiosonde data, we ~~evaluated the quality of the MLH data as observed by the ceilometer and~~ found that the ceilometer underestimates ~~MLH during~~ the MLH under conditions of neutral stratification caused by strong winds, whereas it overestimates ~~MLH during dust crossing. By combining conventional meteorologicaldata and~~ the MLH when sand-dust is crossing. Using meteorological, $PM_{2.5}$, and PM_{10} observational data, we screened the ~~observational results for the MLH , and~~ observed MLH automatically; the ceilometer observations were fairly consistent with the ~~meteorological radiosonde profile results. The correlation coefficient is more~~ radiosondes, with a correlation coefficient greater than 0.9~~, and the effective rate of acquired data is near 80~~. Further analysis ~~of the variation in the MLH indicates~~ indicated that the MLH ~~in the Beijing area exhibits the feature of being~~ is low in autumn and winter and ~~being~~ high in spring and summer in Beijing. There is a significant correlation between the ~~variation in the MLH and the~~ sensible heat flux ~~, whereas the diurnal variation in the mixing layer during summer is~~ and MLH, and the diurnal cycle of the MLH in summer is also affected by the circulation of mountainous plain winds. ~~By applying visibility as the index for the classification of atmospheric pollutiondegree, it is found that in comparison with a clear day, the variation of~~ Using visibility as an index to classify the degree of air pollution, we found that the variation in the sensible heat and buoyancy term in turbulent kinetic energy (TKE) ~~of a slight haze day is insignificant~~ is insignificant when visibility decreases from 10 to 5 km, but the reduction of shear term in TKE is near 70 %~~when visibility decreased from 10 to~~ . When visibility decreases from 5 to 1 km~~; in comparison with the slight haze day~~, the variation of the shear term in TKE ~~of medium and heavy haze days~~ is insignificant, but the ~~declination of~~ decrease in the sensible heat and

buoyancy term in TKE ~~are about~~ is approximately 60 %~~when visibility decreased from 5 to 1~~. Although the correlation between the daily variation of the MLH and visibility is very poor, the correlation between them is significantly enhanced ~~as~~ when the relative humidity increases beyond 80 %. This ~~characterizes the generation of~~ indicates that humidity-related physiochemical processes ~~as the main~~ is the primary source of atmospheric particles under heavy pollution ~~, whereas~~ and that the dissipation of atmospheric particles mainly depends on the MLH. The presented results ~~on~~ of the atmospheric mixing layer ~~and its thermal dynamic structure under different degrees of pollution provide a scientific basis for improving the~~ provide useful empirical information for improving meteorological and atmospheric chemistry models and the forecasting and warning of ~~atmospheric~~ air pollution.

1 Introduction

The mixing layer is formed ~~because of discontinuous turbulence~~ when discontinuous turbulence exists due to discontinuities in temperature stratification between the upper and lower layers ~~resulting from discontinuity in temperature stratification. The height to which the~~ of the atmosphere. The atmospheric mixing layer ~~extends is the mixing layer~~ height (MLH) ~~. The atmospheric MLH~~ is an important meteorological factor that affects ~~atmospheric pollution because it affects~~ the vertical diffusion ~~capability~~ of atmospheric pollutants and water vapour ~~gradients~~concentrations; therefore, it ~~affects the generation~~ impacts the formation and dissipation of air pollutants (Stull, 1988). Continuous observations of the MLH are helpful for improving ~~parameterization schemes of the model boundary layer and beneficial for~~ the parameterisations of boundary layer models, and they play a important role of improving the simulation accuracy of meteorological models and ~~optimizing~~ optimising the simulation results for pollutants.

Three primary observation methods are used to determine the MLH: meteorological ~~sounding profiles~~radiosondes, aeroplane surveys, and ground-based remote sensing. As the most conventional observation approach, meteorological radiosonde profiles ~~have~~ utilise a large number of observation stations distributed globally ~~, and observational~~

~~dataquality is high~~and provide high-quality data. However, because ~~the observational cost is relatively high~~ of the high cost of the observation, only two observations at 00:00 and 12:00 UTC are available from most stations (Seibert et al., 2000). ~~As~~ When solar radiation increases in the morning, the growth rate ~~for~~ of the MLH reaches hundreds of metres ~~to 1000per hour at the stage of fast convection development, and even the hourly observations of the sounding profile could not seize important observational information of~~ per hour and convection develops quickly; even if hourly observations were available, they could not provide sufficient temporal resolution of the evolution of MLH (Seibert et al., 2000). Although aeroplane surveys can be used to obtain high-resolution ~~variations of meteorological and pollutants~~ meteorological and pollutant profiles, the constraints of air traffic control, weather conditions, and observation cost ~~reduce~~ limit these data to ~~a limited time period~~short time periods. Therefore, to acquire continuous observations with high spatial and temporal resolution, ground-based remote sensing has become the most advanced approach ~~for measuring the MLH~~ to MLH measurement.

~~There are three methods of performing ground-based remote sensing: acoustic~~ Acoustic radar (sodar~~– sound detection and ranging~~), laser radar (lidar~~– light intensity detection and ranging~~) and electromagnetic radar (Doppler radar) are the three methods used to perform ground-based remote sensing. Sodar can obtain the vertical ~~profile~~ profiles of wind and temperature~~data; thus, it~~ , and these can be used to ~~further~~ calculate the MLH. Doppler wind radar can obtain variations of the wind vectors at different altitudes and identify the mixing layer through wind shear. Lidar can obtain the vertical profile of ~~variations in~~ the aerosol concentration and discern the atmospheric MLH by calculating the height ~~for sudden changes of aerosol profile. Doppler wind radar can obtain variations in the wind vectors at different altitudes and identify variations in the mixing layer through the wind shear.~~ at which sudden changes in the profile occur.

Beyrich (1997), Seibert et al. (2000), and Emeis et al. (2008) conducted ~~three reviews of the three methodsand compared~~ reviews of these three methods, comparing their advantages and disadvantages. The sodar detection height is usually ~~lower~~ less than 1000 m, which is not conducive for observing the MLH under convection states. ~~Lidar observations~~

~~are usually performed in the visible light band, and it could cause visual hazards when not used properly; moreover, before~~ The lowest detection height of wind radar is normally above 200 m, and the vertical resolution is limited to 50–250 m, factors that make the interpretation of wind radar data not always straightforward (Seibert et al., 2000). Prior to the application of modern laser ceilometers~~for this purpose, lidar observation devices are relatively costly and unlikely to become popularly used. Wind radar is easily interfered by clouds, and the observational height is limited under cloudy conditions.~~ , lidar was costly and not widely used. In recent years, lidar ~~observational~~ observation technology has developed rapidly, and an increasing number of applications have used lidar for MLH observations (White et al., 1999; Steyn, et al., 1999; Hägeli et al., 2000; Chen et al., 2001; Schneider and Eixmann, 2002; Kunz et al., 2002; Strawbridge and Snyder, 2004; He et al., 2006; Wiegner et al., 2006; Sicard et al., 2006; Hennemuth and Lammert, 2006; Emeis et al., 2007; Wang et al., 2012; Yang et al., 2013; Luo et al., 2014; Scarino et al., 2014). ~~Furthermore, the~~ Meanwhile, eye-safe ceilometers ~~CL31 and CL51 have been developed by Vaisala to observe the MLH using~~ that permit observation of the MLH with a near-infrared band laser ~~. Because of the~~ have been developed. Due to their simple operation and low cost, ~~such~~ these instruments have become the optimal ~~solution for observing the MLH~~ method for MLH observation, and they have been ~~applied to an increasing number of observations~~ widely used in recent years (Münkel and Räsänen, 2004; Emeis et al., 2004; Emeis and Schäfer, 2006; Eresmaa et al., 2006; Münkel et al., 2007; McKendry et al., 2009; Kamp and McKendry, 2010; Muňoz and Undurraga, 2010; Flentje et al., 2010; Chen et al., 2011; Haeffelin et al., 2012; Emeis et al., 2012; Pappalardo et al., 2014; Wiegner et al., 2014; Schween et al., 2014; Sicard et al., 2015; Tang et al., 2015).

Beijing, located on the North China Plain, is the centre of politics, culture, and economics in China. ~~Because of the rapid economic development , energy usagehas increased, which has caused~~ With the rapid development of the economy and the concomitant increase in energy usage, serious air pollution and ~~frequent heavy haze days~~ heavy haze occurs frequently (Tang et al., 2009, 2012, 2015; Xin et al., 2010; Wang et al., 2014b; Zhang et al., 2014; Yang et al., 2015). Previous studies of Beijing have indicated that visibility declines

dramatically ~~during heavy pollution periods in Beijing~~ when the concentration of particles increases~~. In addition, ~~; the weather conditions ~~generally include high humidity~~ typically include high relative humidity (RH), stable atmospheric stratification, and low wind speed ~~with a southerly flow , and the atmospheric stratification is stable~~ (WS) with southerly flow during the polluted period (Ding et al., 2005; Liu et al., 2014; Zhang et al., 2015). ~~Previous~~

Although many studies have provided ~~additional descriptions of weather conditions corresponding to~~ detailed descriptions of other weather conditions during heavy pollution periods~~; however, atmospheric MLH variations are the key meteorological factors related to~~ , variations in atmospheric MLH are not well understood. As a key meteorological factor, MLH has a strong influence on the occurrence, maintenance, and dissipation of heavy pollution~~, and they are not well understood. As for~~ . For most areas in ~~north~~ northern China, the meteorological ~~sounding data~~ radiosondes can only acquire ~~observational data for~~ the MLH in the morning (00:00 UTC) and at night (12:00 UTC), ~~and~~ so observations of the convective mixing layer ~~variations~~ at noon are lacking. In certain studies, simulations with numerical models, short-time ground-based remote sensing, or meteorological profiles are used to provide a preliminary description of MLH ~~variations~~ during heavy pollution periods ~~, but continuous high-resolution observations over a long time period have not been conducted for this region~~ (He and Mao, 2005; Yang et al., 2005; Zhang et al., 2006; Chen et al., 2009; Quan et al., 2013; Hu et al., 2014; Zhang et al., 2015)~~. Without acquiring~~ , but continuous high-resolution observations over a long time period have not been conducted for this region. Without the continuous high-resolution ~~variation characteristics of the MLHthrough these studies, the influence of atmospheric~~ characteristics of MLH, its impact on air pollution cannot be studied thoroughly (Schäfer et al., 2006).

To compensate for ~~information gaps~~ the deficiencies in the aforementioned studies, a ceilometer was used to conduct continuous high-resolution observations for 3 years and ~~5~~ 6 months (from July of 2009 to December of 2012) in Beijing. By comparing the obtained data with multiple ~~meteorology~~ meteorological and pollutant data sets, we verified the applicability of the ceilometer and obtained the ~~variation characteristics~~ temporal variations of the MLH over 3 years. By combining the meteorological data, we were able to deter-

mine ~~how variations in~~ the variations of the mixing layer and the atmospheric diffusion capability ~~occurred~~ in different seasons. Finally, ~~visibility was used to determine~~ we used visibility as an index to classify the degree of ~~atmospheric~~ air pollution, and analysed the thermal/dynamic ~~structure~~ parameters inside the mixing layer ~~was analysed~~ under different degrees of pollution~~by delineating~~ ; then, we delineated the influence of MLH ~~variations on atmospheric pollution and revealing~~ on air pollution and revealed the critical meteorological ~~conditions underlying~~ factors that affect the formation and dissipation of heavy ~~atmospheric pollution in the Beijingarea~~air pollution in Beijing.

2 Methods

2.1 Sites and instruments

To understand the ~~structural variations~~ characteristics of the mixing layer in the Beijing area, we conducted observations for 3 years and ~~5~~ 6 months (from 15 July 2009 to ~~31~~16 December 2012) in Beijing. The observation sites, ~~observation~~ parameters, and ~~observation time period~~ time periods are shown in ~~Fig.~~Figure 1 and Table 1.

2.1.1 BJT site

The site used to measure the MLH was built in the ~~tower~~ courtyard of the Institute of Atmospheric Physics, Chinese Academy of Sciences, to the west of the Jiande bridge in the Haidian district, Beijing (ID: BJT). This site is located between the north third ~~ring road and~~ and the north fourth ring road, and the Beijing–Tibet motorway is on the eastern side. The geographic location of the station is ~~39.97~~39.974° N, ~~116.37~~116.372° E, and the elevation (a.s.l.) is approximately 60 m.

The instrument used to observe the MLH was a single-lens ceilometer ~~CL31 (Vaisala~~(CL31, Vaisala, Finland). This instrument ~~utilizes~~ utilises pulsed diode laser lidar technology (910 nm waveband) to measure the attenuated backscatter coefficient profile ~~of atmospheric aerosols~~ and then determine the MLH. ~~In practical measurementsusing the~~

~~CL31~~For practical measurements, the time resolution was set to 16 s, the vertical resolution was set to 10 m, and the measurement range was 7.7 km. Because the atmospheric aerosol concentration is relatively high in Beijing, the CL31 lens was cleaned with clear water every 3 days.

The conventional meteorological data during the same period ~~were from temperature, humidity, wind speed~~included temperature, RH, WS, and wind direction observations at 8, 15, 32, 47, 65, 80, 100, 120, 140, 160, 180, 200, 240, 280, and 320 m ~~up the tower~~ along the tower in a vertical direction, and the temporal resolution was 5 min. ~~A~~ The detailed description is provided by Song et al. (2013). The thermodynamic ~~parameter data in the atmospheric mixing layer~~ parameters (sensible heat, latent heat, ~~radiation,~~ friction velocity, etc.) and the total (285-2800 nm) and net (0.2-100 µm) radiation during the same period were ~~from ultrasonic anemometers at 47, 140 and 280~~observed using a ultrasonic anemometers (CSAT3, Campbell Scientific, USA), a pyranometer (CM11, Kipp & Zonen, Netherlands) and a net radiometer (NR Lite2, Kipp & Zonen, Netherlands), respectively. All of these data were obtained on the meteorological tower ~~, and the time resolution was 5~~at a height of 280 m and processed with a resolution of 30 min. ~~A~~ The detailed description is provided by Hu et al. (2012) and Song and Wang (2012). The ~~observation data of~~ sensible heat (Q_H), latent heat (Q_E), friction velocity (u_*), and turbulence kinetic energy (TKE) were calculated as follows (Stull, 1988; Garratt, 1992):

$$Q_H = \rho c_p \overline{w'\theta_v'} \tag{1}$$

$$Q_E = L_v \overline{w'q'} \tag{2}$$

$$u_* = \left(\overline{u'w'}^2 + \overline{v'w'}^2\right)^{1/4} \tag{3}$$

$$\frac{TKE}{m} = \frac{1}{2}\left(\overline{u'^2} + \overline{v'^2} + \overline{w'^2}\right) = \overline{e} \tag{4}$$

where ρ is the air density ($kg\,m^{-3}$), c_p is the specific heat capacity for air at constant pressure ($J\,kg^{-1}\,K^{-1}$), θ_v is the virtual potential temperature (K), L_v is the latent heat of vaporisation of water ($J\,kg^{-1}$), q is the water vapor density ($kg\,m^{-3}$), m is the mass (kg), $\overline{e}$ is the TKE per unit mass ($m^2\,s^{-1}$), and u, v, and w are the streamwise, cross-stream and vertical wind velocities ($m\,s^{-1}$), respectively.

To identify the sand-dust crossing, the ratio of $PM_{2.5}$ and PM_{10} was used as an index. If there was no sand-dust crossing, the ratio of $PM_{2.5}$ to PM_{10} might almost exceed 50 % (Liu et al., 2014). A sudden decrease in the ratio to 30 % or lower and PM_{10} concentration higher than 500 $\mu g\,m^{-3}$ usually indicate a sand-dust crossing. The ground observations of $PM_{2.5}$ and PM_{10} during the same period were ~~from Thermo Electric Inc.~~ made by the ambient particulate monitor (RP1400a~~), and the time resolution was~~ , Thermo Fisher Scientific, USA). The data were acquired at a time resolution of 5 min and processed with a resolution of 60 min. A detailed description is provided by Liu et al. (2014).

~~The meteorological sounding profile data~~

2.1.2 ZBAA site

The meteorological radiosondes were measured by the international standard weather station (ID: ZBAA) ~~, which~~ that is located outside the south second ring road in the Fengtai district, Beijing, 10 km from the station ~~on the tower~~ of the Institute of Atmospheric Physics. The geographic position of station ZBAA is ~~39.48~~39.484° N and ~~116.28~~116.282° E, and the elevation (a.s.l.) is approximately 34 m. ~~The meteorological sounding profile data~~

The meteorological radiosondes observed at station ZBAA included two categories: conventional observations, which were conducted at 08:00 LT in the morning and at 20:00 LT in the evening each day; and intensified observations, which were conducted at 14:00 LT in the afternoon every Thursday. The observed meteorological parameters included atmospheric pressure, temperature, ~~wind speed,~~ RH, WS, wind direction, and ~~humidity. According to the classification method~~ ozone. In this study, the methods of Eresmaa et al. (2006) ~~, we defined all of the meteorological sounding profiles as a convection~~ and Münkel et al. (2007) were used to divide the radiosondes into stable and convective states

according to the atmospheric stratification status. The meteorological radiosondes were defined as encountering a convective state when they exhibited negative lapse rates for the ~~virtual potential temperature~~ θ_v within 200 m and bulk Richardson ~~number~~ numbers (R_B) within 100 m, and ~~the~~ other profiles were defined as a stable state. ~~We obtained 260 and 540 effective observation samples for the two types of weather conditions, respectively. In order to characterize~~ In this project, the R_B was determined by the formula of Stull (1988), as follows:

$$R_B = \frac{g\Delta\theta_v\Delta z}{\theta_v\left((\Delta u)^2 + (\Delta v)^2\right)} \tag{5}$$

where g is the acceleration of gravity ($m\,s^{-2}$), and z is the height (m).

PM concentration proved to be a good indicator for characterization of the degree of ~~the air pollutionin Beijing, visibility~~ air pollution. However, haze was defined by the visibility in China as shown in Table 2 (CMA, 2010), and it was remarkably negatively correlated with PM concentration (Yang et al., 2015). Because PM data were occasionally missing, visibility was used as an index to classify the degree of air pollution. Visibility at station ZBAA, which was obtained from the ~~web page of Wyoming EngineeringUniversity ()~~Department of Atmospheric Science, College of Engineering, University of Wyoming (http://weather.uwyo.edu/surface/meteorogram/), was measured by a visibility sensor (PWD12, Vaisala, Finland) with an accuracy of $\pm$ 10 %.

2.2 Determination of the MLH

2.2.1 MLH retrieval by ceilometer

Because the lifetime of particles ~~is relatively long and could~~ can be several days or even weeks, the distribution of particle concentrations ~~inside the atmospheric mixing layer is even more uniform compared with~~ in the MLH is more uniform than that of gaseous pollutants. However, the particle concentration in the mixing layer and ~~free atmosphere is~~ that in the

free atmosphere are significantly different. ~~By analysing~~ In the attenuated backscatter coefficient profile~~of atmospheric particles~~, the position at which a sudden change occurs in the ~~attenuated backscatter coefficient is~~ profile indicates the top of the atmospheric mixing layer. In this study, we used the gradient method to determine the MLH by selecting the location with the maximum negative gradient ($-\mathrm{d}\beta/\mathrm{d}x$) in the attenuated backscatter coefficient profile ~~diagram for the aerosol~~ as the top of the mixing layer (Steyn, et al., 1999). To eliminate the influence of inherent noise and aerosol ~~layer structure influence~~ layers on the data, spatial and temporal averaging must be ~~applied~~ carried out before the gradient method ~~can be used to calculated the MLH from the profile data~~ is used to calculate the MLH (Münkel et al., 2007; Tang et al., 2015). Time averaging is dependent on the current signal noise; the intervals vary from 14 to 52 min for the CL31. Height averaging intervals range from 80 m at ground level to 360 m at 1600 m height and beyond. Additional features of this algorithm, which is used in the Vaisala software product BL-VIEW, are cloud and precipitation filtering and outlier removal.

2.2.2 MLH retrieval by radiosonde

A number of methods have been developed ~~to analyse~~ for analysis of the mixing layer through the meteorological ~~sounding profile~~ radiosonde (Beyrich, 1997; Sibert et al., 2000; Wang and Wang, ~~2014~~2014a). In this study, we calculated the MLH for the convective ~~state and stable state~~and stable states, respectively. For the convective state, we used the Holzworth method (Holzworth, 1964, 1967), which is the method most widely applied to obtain the MLH by analysing ~~variations in the virtual potential temperature~~profiles in the θ_v. In a stable state, a low-level jet often occurs in ~~the Beijingarea~~Beijing, and we can determine the MLH by analysing the position of the low-level jet (Tang et al., 2015). If the low-level jet does not ~~occur~~ exist under stable weather conditions, the altitude ~~where the Richardson number~~ at which the R_B is greater than 1 is the MLH (Vogelezang and Holtslag, 1996; Eresmaa et al., 2006).

3 Results and discussions

3.1 Verification of the MLH

Previous ~~observation studies using ceilometers could~~ studies with ceilometers did not resolve issues ~~with applying~~ concerning the applicability of ceilometers in Chinese areas with high aerosol concentrations. ~~In this study, the methods of Eresmaa et al. (2006) and Mnkel et al. (2007) were used to divide the samples into stable and convective states according to the atmospheric stratification status~~According to the methods described in Sect. 2.1.2, 260 and 540 effective observations were obtained for the convective and stable states, respectively. The MLH data acquired by meteorological ~~sounding profiles and the~~ radiosondes and by ceilometer were compared for the two types of weather conditions (Fig. 2)~~, and the results were evaluated. The comparative analysis~~ . Using the MLH calculated by the radiosondes as a reference, the comparison showed that the MLH observed ~~by~~ from the ceilometer was overestimated ~~and~~ or underestimated in a portion of the samples.

Because the ceilometer determines the MLH by measuring the attenuated backscatter profile~~of atmospheric particles~~, if the concentration of atmospheric particles is relatively low, ~~then the height measurement errors of the mixing layer will increase correspondingly (~~it will be difficult to determine the MLH based on a sudden change in the backscatter profile, and use of this method will lead to a higher absolute error (AE) of the measured MLH (Eresmaa et al., 2006; Muñoz and Undurraga, 2010). ~~An analysis of the relationship between the visibility and comparison results showed that underestimations in the ceilometer observation results generally corresponded with good visibility and low aerosol concentrations. Nevertheless, among the samples with relatively good visibility,~~ When taking the visibility into account, we found that the underestimations of the observed MLH always occurred when visibility was good. However, there were still a number of samples ~~had relatively low errors~~ that had low AE under conditions of good visibility (Fig. 2). Consequently, ~~low pollution and~~ clear days with good visibility are not ~~sufficient conditions to~~

predict underestimations in the observation resultsthe main reason for underestimation of the observed MLH.

To investigate why the ceilometer results produced underestimations, we analysed cases with low aerosol concentrations and small measurement errors and found that when there was a large difference in the aerosol concentration between the near surface and high altitude, the calculation error those samples with good visibility and small AE. The results showed that although the visibility was good, the AE of the MLH decreased, even if was still small when the aerosol concentration was relatively low. By further analysing the relationship between the ceilometer and meteorological sounding profile results with the relative humidity and wind vectors showed large differences in the vertical direction. After taking the RH and wind vectors into account, we found that ceilometer underestimations corresponded with low relative humidity and large wind speed, with winds mostly from the north underestimations were always accompanied by low RH and strong northerly wind (Figs. 3 and 4). The local meteorological conditions in Beijing indicated that this type kind of meteorological condition is usually caused by a the bypass of a cold air mass. When a strong northerly winds are dominant over Beijing, with a dry and clear air masses prevail, and the large wind speed causes the atmospheric aerosols to rapidly spread prevails in Beijing, atmospheric aerosols spread rapidly to the downstream region, resulting in a dramatic decrease of aerosol concentration in local aerosol concentration and good visibility. In addition, the low humidity of the dry air mass suppresses the liquid-phase and heterogeneous reactions for of the gaseous precursors of aerosol, and the hygroscopic growth of aerosols can also be neglected. Therefore, the aerosol generation velocity is much lower than the loss rate because of transportationformation of aerosols cannot compensate for the transportation loss, leading to low aerosol concentrations and uniform vertical gradientsand uniform aerosol concentrations in the vertical direction. Once the aerosol concentrations in vertical direction become uniformconcentration becomes uniform in the vertical direction, the ceilometer cannot calculate the MLH through sudden changes in the attenuated backscatter profile, which results profiles, resulting in serious underestimations. An analysis of the relationship between the Richardson number and the error shows

R_B and the AE showed that when the ceilometer-measured MLH is subject to ~~relatively large errors, the Richardson number is approximately 0. Therefore~~large AE, the R_B below 100 m is approximately 0 (Fig. S1). Thus, the near-neutral atmospheric stratification ~~that occurs when~~ caused by the passage of a cold air mass ~~passes through is the main cause~~ is the primary reason for the serious ~~underestimation in the observation results by the ceilometer~~underestimations.

~~To investigate the overestimations in~~ With respect to overestimations of the ceilometer results, ~~an analysis of the observation results for the particle concentration showed that in this situation, the concentration is relatively low, but the concentration is relatively high (Fig. 2). To investigate the reason of the overestimations, we used the meteorological sounding profile~~ we may take the meteorological radiosonde at 14:00 LT on ~~19~~29 December 2009 as an example ~~and analysed it for overestimations~~ (Fig. 5). ~~This profile exhibited an obvious bi-level structure, with the first level~~ The MLH is determined at approximately 1100 m~~; where the virtual potential temperature begins to gradually increase, the wind speed begins to increase, and~~ , where the θ_v and the WS begin to increase; the ozone concentration is transported from the background area~~with a concentration of about~~ , where ozone is present at approximately 40 ppbv. ~~The second level is~~ However, the ceilometer recorded a higher MLH at approximately 1600 m, where ~~the variation rate of virtual potential temperature increases. However, the ceilometer-measured attenuated backscatter coefficient profile cannot resolve this type of bi-level structure. A ratio of~~ there was a sudden change in the backscatter gradient. When we measured the $PM_{2.5}/PM_{10}$ ratio at this moment, we found that the ratio was only 0.15~~exhibits clear characteristics of dust crossing. Therefore, the aerosol concentration caused by this type of dust crossing is uniform in the vertical direction below the second layer for the ceilometer, whereas the presence of obvious wind shear and sudden virtual potential temperature changes for the radiosondes are the main reasons for the overestimated observation results by the ceilometers~~ , a clear characteristic of a sand-dust crossing. Due to the large number of dust particles, the aerosol concentrations became uniform below 1600 m. This led to a sudden change in the backscatter gradient at 1600 m and made it difficult to identify the real MLH at 1100 m; thus, an erroneously high

MLH was determined. This result shows that sand-dust crossing is the main reason for the overestimations (Figs. 2 and 5).

Because the detected aerosol layers are not only the result of ongoing vertical mixing but also always originate from advective transport or past accumulation processes, interpreting data from aerosol lidars is often not straightforward (Russell et al., 1974; Coulter, 1979; Baxter, 1991; Batchvarova et al., 1999). Therefore, improving the algorithm cannot resolve the underestimations and overestimations of the ceilometer observations; the only option that can be used to rectify the MLH is to eliminate the data with large AE. After determining the reasons for the underestimations and overestimations~~in the ceilometer data, the results with large errors according to certain principles must be eliminated~~, the elimination is much easier to implement. For underestimations, the meteorological data ~~at the observation station~~ were used to eliminate ~~time periods of crossing cold air when the temperature and wind velocity are subject to~~ the periods when cold air passed with a sudden change in temperature and WS. For overestimations, we ~~used the date of dust occurrence based on the sand–dust~~ referred to the sand-dust weather almanac to ~~eliminate the time periods of dust crossing when the~~ identify the sand-dust days firstly (CMA, 2012, 2013, 2014, 2015). Using the principal described in Sect. 2.1.1, the exact times of sand-dust starting and ending were determined as the times which the the ratio of $PM_{2.5}$ ~~and to~~ PM_{10} suddenly ~~decreases. An analysis of the meteorological sounding profiles after eliminating the erroneous data showed that a high correlation occurred between the~~ decreased or increased, respectively. Finally, the data obtained during the sand-dust periods were eliminated.

After the screening process, the post-elimination ceilometer data and meteorological ~~sounding observations, and the correlation coefficient was more~~ radiosondes are strongly correlated, with a correlation coefficient greater than 0.9, ~~which also demonstrated the effectiveness and manipulability~~ demonstrating the effectiveness of the elimination method (Fig. 6). ~~Overall, by analysing the weather conditions that caused the error of ceilometer observation, the conventional meteorological data and and were used to eliminate the observation results. The~~ Consequently, the elimination results are good~~, and this~~ . This

method replaces the time-consuming method of filtering the data manually ~~, which~~ and is of great practical value for future measurements of MLH with ceilometers.

3.2 MLH variations

To provide a detailed description of variations in the MLH, we selected ~~high-quality~~ continuous measured MLH and meteorological data ~~in 3 consecutive years~~ over a 3-year period (from December 2009 to November 2012). First, the ~~effectiveness of the data must be verified after performing the~~ availability was verified after the MLH elimination by the aforementioned method. The results of the evaluation indicate that the ~~effectiveness of the data~~ availability in different seasons is significantly negatively correlated with ~~wind speed and significantly~~ WS and positively correlated with ~~relative humidity~~ RH (Fig. 7a). For spring and winter seasons with ~~relatively large wind speeds and relatively low humidity, the effectiveness of the data~~ large WS and low RH, the availability is low, whereas for summer and autumn seasons with ~~relatively small wind speeds and relatively high humidity, the effectiveness of the data~~ small WS and high RH, the availability is high. In particular, the ~~effectiveness~~ availability is lowest in January at 63.5 % and highest in June at 95.0 %. The ~~average effectiveness of the data over 3 years~~ successful retrieval of MLH over the 3-year period is approximately 80 %, much higher than in a previous study (Muňoz and Undurraga, 2010).

Using the validated data, we ~~analysed seasonal changes~~ analyzed seasonal variations over 3 years. The results ~~indicated that the daily minimum~~ showed that the changes of the monthly mean were similar in different years, and no inter-annual trend can be found (Fig. S2). Therefore, we examined the averaged seasonal variation, and the monthly mean of the daily minimum, average, and maximum were calculated, respectively. The daily minimum of the mixing layer was high in winter and ~~in~~ spring, and low in summer and ~~in~~ autumn. The ~~monthly average maximum for~~ maximum monthly mean of the daily minimum MLH ~~of~~ was 351 $\pm$ 185 m ~~appeared~~ in May, and the minimum ~~of~~ was 238 $\pm$ 202 m ~~appeared~~ in October. The daily minimum MLH generally occurred during night-time ~~with~~ under conditions of stable stratification, and the nocturnal stable boundary layer height was

closely related to ~~wind speed~~ WS (Zilitinkevich and Baklanov, 2002; Hyun et al., 2005); therefore, the seasonal variation in daily minimum MLH was consistent with the seasonal variation in ~~wind speed~~ WS (Fig. 7a).

Compared with the ~~average~~ daily minimum MLH, both the monthly mean of the daily average and the ~~average daily~~ maximum MLH exhibited different seasonal variations. As shown in Fig. 7b, two platform periods ~~and~~ (from March to August and from October to January) and two transitional periods (February and September) occur for the ~~variations of the~~ monthly average MLH. The MLH is similar ~~in October and November (autumn) and January and December (winter) at~~ from October to January at approximately 500 m, and it is similar ~~in March , April, and May (spring) and June, July, and August (summer) at~~ from March to August at approximately 700 m. February and September are the two transitional months and have values of approximately 600 m. The month with the highest MLH is May at 739 $\pm$ 137 m, and the MLH is lowest in December at 435 $\pm$ 148 m. The seasonal variation in the ~~average~~ daily maximum MLH is similar to the monthly ~~average. The monthly average daily maximum MLH is~~ mean with the highest in May at 1480 $\pm$ 448 m ~~, and is~~ and the lowest in December at 787 $\pm$ 297 m.

Previous studies have ~~indicated~~ suggested that the seasonal variation in the MLH ~~could~~ may be related to ~~the~~ radiation flux (Kamp and McKendry, 2010; Muňoz and Undurraga, 2010)~~. As~~ , but our study was not entirely consistent as shown in Fig. 7b~~, the total radiation flux during spring in Beijing is significantly higher than in summer, whereas~~ . Although spring had a significantly higher total radiation flux than summer, the MLH in ~~summer~~ spring is equal to that in ~~spring, and this result is inconsistent with that of previous studies. Although this study has determined seasonal variations in the MLH,~~ summer. This is because more data were eliminated for winter and spring, especially for weather with dry wind and relatively high MLHs~~,~~. Thus, using the monthly mean of MLH is not a good method by which to analyse the reasons for MLH variations.

To gain a better understanding of the ~~monthly means of MLH in winter and spring seasons were likely underestimated. To avoid the influence of data elimination on the study, we analysed the relationship between daily changes of the mixing layer and the sensible heat~~

~~flux and found~~ MLH variations, we use the daily mean instead of the monthly mean to do the analysis. As the most simple framework in which we can analyse the MLH variations in Beijing, we consider the thermodynamic model of the mixing layer growth (Stull, 1988), as follows:

$$\frac{\partial z_i}{\partial t} = \frac{\overline{w'\theta'_s} - \overline{w'\theta'_{z_i}}}{\gamma z_i} \tag{6}$$

where z_i is the MLH (m), t is the time (s), θ_s is the virtual potential temperature near the ground (K), θ_z is the virtual potential temperature in the top of the mixing layer (K), and γ is the lapse rate of the virtual potential temperature (K m^{-1}). Suppose the heat from the ground is the only way to warm the mixing layer and the heat flux at height z_i is zero, then the MLH is related to $\overline{w'\theta'_s}$. Considering that Q_H is defined as the equation (1), MLH is correspondingly related to Q_H. Therefore, the relationship between daily changes in the Q_H at 280 m and MLH was analysed. The results showed that the average Q_H and MLH from 12:00 to 17:00 LT ~~and the sensible heat flux~~ were well correlated~~and had~~, with a correlation coefficient of 0.65~~, which characterizes the~~. Because net radiation (Q^*) should be balanced by the Q_H, Q_E, and soil heat flux (Q_G) given as follows (Stull, 1988):

$$Q^* = Q_H + Q_E + Q_G \tag{7}$$

the strong correlation between the Q_H and MLH proves the dominant role of radiation in the ~~variations~~ variation of MLH (Fig. 8).

3.3 Impact of mountainous plain winds on MLH

We analysed the diurnal variations ~~in~~ of MLH on a monthly basis and found that the MLH develops in four stages: from 09:00 to 14:00 LT, which is the fast development stage~~for the MLH~~; from 14:00 to 18:00 LT, which is the maintenance stage~~of the mixing layer~~; from 18:00 to 20:00 LT, which is the rapid decrease stage~~of the mixing layer; and after~~ ; and from

20:00 LT ~~and until~~ to the next morning at 08:00 LT~~in the morning of the second day~~, which is the stable boundary layer stage ~~with relatively low MLH~~ (Fig. ~~9a~~S3). These ~~types~~ stages of development and dissipation mechanisms are consistent with the description ~~of~~ reported by Stull (1988). ~~Although the daily~~ The daily MLH range is 728, 828, 562, and 407 m for spring, summer, autumn and winter, respectively. The relatively low ranges in autumn and winter are obviously related to the low radiation flux. However, it should be noted that summer has lower radiation and a larger daily range than spring (Fig. 7). Therefore, our study will emphasise the reasons for the differences in the daily MLH range in summer and spring.

As shown in Sect. 3.2, the monthly average MLH is ~~close~~ similar between spring and summer~~, the diurnal variation in the MLH exhibits considerable differences. At~~ . However, when the daily growth rates in spring and summer were compared using the T test, the results showed the difference was significant (P<0.05) between the two seasons. As shown in Figure 9a, at night-time in spring, the MLH is high and ~~relatively stable~~almost constant, whereas at night-time in summer, the MLH ~~exhibits~~ shows a gradual decreasing trend. After sunrise and before 12:00 LT, the ~~growth rate of the atmospheric~~ rate of increase in the MLH is relatively high in spring~~and reaches~~ , reaching 114 m h^{-1}, whereas the ~~hourly growth rate of the mixing layer~~ rate in summer is relatively low~~in summer and only reaches~~ , 102 m h^{-1}. Between 12:00 and 14:00 LT in spring, the ~~growth rate of~~ rate of increase in the MLH is 119 m h^{-1}, whereas ~~the growth rate of the MLH~~ in summer the rate of increase is significantly enhanced~~in summer and reaches~~ , reaching 165 m h^{-1}. Such changes reflect the convex ~~variation characteristics in spring~~ and concave characteristics in spring and summer during the development stage of the MLH, respectively.

~~According to the description in Sect. 3.2, variations in the MLH should exhibit a good linear relationship with the amount of radiation. Because of the relatively high radiation in spring, the relatively high MLH variation for days with lower radiation in summer is difficult to explain with the radiation flux, which indicates that there are other factors that affect the characteristics of the MLH variation. Because the MLH is affected by many factors, its development is~~ The development of MLH is mainly related to the ~~magnitude of turbulent energy. Two components are~~ turbulent energy and the production of the turbulent energy

is closely related to ~~turbulent energy~~two components: the heat flux caused by radiation ($\frac{g}{\theta_v}\overline{w'\theta'_v}$) and the momentum flux generated by wind shear ($-\overline{u'w'}\frac{\partial \overline{u}}{\partial z}$) (Stull, 1988). Because the seasonal variation ~~of~~ in heat flux is difficult to explain ~~according to the aforementioned criteria~~the daily MLH range, we analysed the seasonal variations ~~in~~ of the horizontal wind vector~~at Beijing station.~~ .

To avoid the impact of near-surface buildings on the wind measurements, we selected the wind vector at 100 m on the Beijing tower. Figure 9b shows that there is ~~an~~ obvious seasonal variation ~~in~~ of the wind vector~~of the Beijing area. The~~ . In winter and spring, Beijing is affected by the Siberian High; at these times, a strong prevailing northwest wind with dry air mass always occurs. Therefore, winter season is dominated by a northwesterly wind, whereas ~~the spring season~~ spring typically exhibits a ~~northwesterly~~ northwest wind in the morning and ~~southwesterly~~ a southwest wind in the afternoon. ~~What matters most is that the alternation phenomenon between the mountainous wind beginning at 03:00at night and the valley wind at 12:00in the afternoon starts to occur in summer. From September, the circulation of mountainous plain wind slowly weakens, and this regional circulation essentially disappears in November. Beijing is affected by the Siberian High in winter and spring, a prevailing northwest wind and dry air mass with relatively large wind velocity occur. However, the~~ In summer, the northward lift and westward intrusion of a subtropical high ~~in summer~~ causes the southerly moist air mass with ~~relatively small wind velocity to~~ small WS to arrive and dominate. Because Beijing is located ~~to the~~ west of the Taihang Mountains and south of the Yanshan Mountains ~~, in the absence~~ (Fig. 1), without the passage of large- or medium-scale meteorological systems ~~passing through in~~ in the summer, the local mountainous plain wind is superimposed ~~to~~ on the southerly air flow and ~~jointly affects~~ these two systems jointly affect the meteorological characteristics of the North China Plain. Therefore, the alternation between the mountainous winds that begin at 03:00 LT at night and the plain winds that begin at 12:00 LT in the afternoon occurs in summer. In September, with the southward and eastward movement of the subtropical high, the circulation of mountainous plain winds starts to weaken, and this circulation disappears in November.

When this regional circulation occurs along with surface cooling that occurs at night in summer, the cold air near the surface forms a shallow down-sliding flow from the northeast to the southwest~~, and this is called the downslope wind or cold drainage flow. The cooled air then~~ . The cold air flows into the ~~plain~~ North China Plain and accumulates in a cold pool, ~~and the cold air that continuously fills the plain continues to increase the~~ increasing the thickness of the inversion layer, and the thickness of the mixing layer gradually decreases. After sunrise~~as the radiation enhances, the~~ , the radiation increases; the MLH increases rapidly under the impact of thermal buoyancy lift~~causes the MLH to increase rapidly~~, and this type of cold drainage flow is maintained until 12:00 LT. After 12:00 LT, the plain wind ~~in~~ from the southwesterly direction gradually dominates and is maintained until approximately 03:00 LT in the morning of the ~~second~~ next day. According to Fig. 9c, from 03:00 LT to 12:00 LT ~~during~~ in summer, the ~~air space from the near surface to~~ troposphere below 300 m ~~is gradually controlled by~~ gradually cools down from low to high due to the cold drainage flow in the northeasterly direction, and the MLH exhibits a gradually ~~diminishing~~ decreasing trend from 03:00 to 06:00 LT. ~~This~~ However, this trend does not occur in spring (Fig. 9a). Similarly, between 09:00 and 12:00 LT in summer, the cold drainage flow ~~causes~~ suppresses the development of the MLH with a low ~~hourly growth rateof the mixing rate in summer, whereas~~ growth rate; in spring, without this inhibitory effect, the growth rate of the MLH is high~~in spring~~. After 12:00 LT in summer, the southerly plain wind causes the growth rate ~~of the MLH to increase from~~ to increase between 12:00 ~~to~~ and 14:00 LT~~in summer. The gradual reduction of the night-time mixing layer and the relatively low rising velocity after sunrise demonstrate the inhibitory effect of this cold drainage flow on the development of the MLH.~~ .

In summary, the mountainous wind in summer causes the mixing layer to ~~gradually decline at night, which~~ decline gradually at night; this also suppresses the development of the mixing layer before noon, and the prevalence of plain winds after noon causes the mixing layer to increase rapidly. Therefore, ~~this regional circulation leads to the~~ compared to the spring, the regional circulation in summer produces a concave-down variation in the

~~fast~~ rapid development stage of the ~~mixing layer in summercompared to the spring~~MLH in summer.

3.4 Implications for air pollution

3.4.1 Thermal/dynamic ~~structures inside mixing layers with~~ parameters under different degrees of pollution

To analyse variations in the thermal dynamic parameters inside atmospheric mixing layers under different degrees of pollution, visibility was used ~~to indicate the degree of atmospheric pollution. Variations in atmospheric visibility were used in the statistical analysis of the thermal dynamic parameters in the atmospheric mixing layer, and variation features were obtained for the wind speed, humidity, sensible heat, latent heat, friction velocity, and turbulent kinetic energy (TKE)~~ as a reference. WS, RH, Q_H, Q_E, u_*, and $\overline{e}$ at 280 m were obtained under different visibility conditions ~~. As shown in~~ (Tab. 2 and Fig. 10). Clear days were defined as days when the visibility is ≥ 10 km, and slight, light, medium, and heavy haze pollution corresponded with 5 km $\leq$ visibility $<$ 10 km, ~~on~~ 3 km $\leq$ visibility $<$ 5 km, 2 km $\leq$ visibility $<$ 3 km and visibility $<$ 2 km, respectively (CMA, 2010). On clear days with atmospheric visibility $\geq$ 10 km, ~~the relative humidity~~ RH was the lowest, with an average of 43.3 %, ~~whereas the sensible heat flux, friction velocity and TKE~~ and Q_H, u_* and $\overline{e}$ were the highest~~and averaged~~ , averaging 20.4 W m^{-2}, 0.45 m s^{-1}, and 0.99 m^2 s^{-2}, respectively. The MLH was ~~664.2~~664 m on average, and the maximum ~~after noon could reach 1144.8~~in the afternoon reached 1145 m~~. With declines of atmospheric visibility, slight haze pollution occurred in the visibility range of 5 to 10(CMA, 2010)~~. Compared with clear days, ~~the relative humidity~~ during light haze pollution the RH significantly increased to 63.1 %, and ~~both the friction velocity and TKE~~ the u_* and $\overline{e}$ significantly declined to 0.32 m s^{-1} and 0.64 m^2 s^{-2}, respectively, ~~at~~ with a reduction ~~rate~~ of approximately 30 %~~, whereas the average sensible heat flux and MLH did not show significant changes at values of~~ ; the Q_H and MLH was 19.7 W m^{-2} and ~~671.0~~671 m, respectively~~. As the atmospheric visibility continued to decline, light haze pollution occurred in the visibility range of 3 to 5, medium haze pollution~~

~~occurred in the visibility range of 2 to 3, and heavy haze pollution occurred in the visibility range of less than 2(CMA, 2010). Compared with slight haze pollution conditions, the relative humidity~~ , without any significant changes. With the pollution aggravated, the RH continued to increase~~with the aggravated pollution, and in the periods of~~ ; during light, medium, and heavy haze it ~~could reach~~ reached to 73.4, 79.6, and 86.4 %, respectively~~; the friction velocity~~ . The u_* and $\overline{e}$ remained almost constant, and the Q_H and MLH showed significantly declining trend. The measured values under light, medium, and heavy haze were as follows: u_* was 0.28, 0.26, and 0.23 $m\,s^{-1}$, respectively; ~~the TKE~~ $\overline{e}$ was 0.56, 0.52, and 0.46 $m^2\,s^{-2}$, respectively; ~~the sensible heat flux~~ Q_H was 15.2, 12.8, and 7.8 $W\,m^{-2}$, respectively; and the MLH was ~~586.1, 430.0, and 320.1~~586, 430, and 320 m, respectively. ~~Therefore~~

In summary, when clear days change to slight haze, the ~~wind speed, friction velocity, and TKE significantly decline but the sensible heat flux~~ WS, u_*, and $\overline{e}$ decline significantly but the Q_H and MLH do not change significantly. When ~~the degree of pollution transforms from slight haze~~ slight haze evolves to light, medium, and heavy haze, significant changes in u_* and $\overline{e}$ do not occur~~in the friction velocity and TKE, the sensible heat flux significantly declines, and the MLH gradually decreases~~, but the Q_H and MLH decrease significantly. It should be noted that although the ~~relative humidity~~ RH varied considerably at different pollution stages, significant ~~differences~~ changes in Q_E did not occur~~in the latent heat flux, which varied from clear days to heavy haze days at~~ ; its values was 18.7, 19.9, 21.5, 18.8, and 19.8 $W\,m^{-2}$ on clear days and under conditions of slight, light, medium, and heavy haze,respectively. Thus, when clear days ~~transform~~ change to slight haze, dynamic effects have a relatively large ~~influence~~ impact on the mixing layer, whereas ~~thermodynamic effects have a relatively significant influence during the transition process from slight haze~~ when slight haze evolves to heavy haze, thermodynamic effects play a dominant role.

To verify these results, we examined the TKE budget equation. If we presume a horizontal average and neglect the advection of wind, ~~then~~ the forecast equation of the TKE can be

written as follows (Stull, 1988; Garratt, 1992):

$$\frac{\partial \overline{e}}{\partial t} = -\overline{u'w'}\frac{\partial \overline{u}}{\partial z} + \frac{\partial g}{\partial \overline{\theta_v}}\frac{g}{\overline{\theta_v}}\overline{w'\theta_v'} - \frac{\partial\left(\overline{w'e} + \frac{\overline{w'p'}}{\rho}\right)}{\partial z}\frac{\partial\left(\overline{w'e}\right)}{\partial z} - \frac{1}{\rho}\frac{\partial\left(\overline{w'p'}\right)}{\partial z} - \varepsilon, \quad (8)$$

where ~~θ_v is the virtual potential temperature~~p is the air pressure (Pa), and ε is the dissipation term of TKE ($m^2\,s^{-3}$). The first term on the right side of the equation is the production and loss term caused by wind shear~~, ~~; the second term ~~on the right side of the equation~~ is the buoyancy production and depletion term, ~~the third term on the right side of the equation is the~~ and the third and fourth terms are the turbulent transport and pressure-related ~~term, and the last term on the right side of the equation is the dissipation term. The turbulent transportation~~ terms, respectively. Because the turbulent transport term does not generate or destroy the TKE ~~, and it just~~ but simply moves the TKE from one position to another ~~position or redistributes~~ or redistributes it, the integral of this term in the ~~TKE. This term remains constant at zero in the entire mixing layer ; therefore, we did not analyse it in this study~~mixing layer remains constant at zero. Moreover, because the time period of pollution usually corresponds to the stable state, the pressure-related term is also small at this time. Therefore, ~~to~~ we did not consider the third and fourth terms of TKE in this study.

To differentiate the contribution of horizontal ~~turbulence~~ and vertical turbulence to the TKE, ~~we only analysed~~ the shear and buoyancy ~~term in~~ terms in the TKE forecast equation were analysed as in the previous study (Ye et al., 2015). As shown in Fig. 10d, the ~~average value of the buoyancy term for~~ buoyancy term on clear days, slight~~haze, lighthaze, mediumhaze~~, light, medium, and heavy ~~haze~~ hazy days is 0.67×10^{-3}, 0.64×10^{-3}, 0.49×10^{-3}, 0.39×10^{-3}, and $0.24 \times 10^{-3}\ m^2\,s^{-3}$, respectively, and the ~~average shear term~~ shear term under these conditions is 1.02×10^{-3}, 0.66×10^{-3}, 0.37×10^{-3}, 0.26×10^{-3}, and $0.23 \times 10^{-3}\ m^2\,s^{-3}$, respectively. Therefore, the key meteorological factor for the conversion from clear ~~days to slight haze is the~~ to slight hazy days is the decrease of the shear term in TKE, and it is mainly ~~characterized~~ characterised by a significant reduction ~~of~~ in the horizontal wind velocity; ~~the key meteorological factor~~ for the

conversion from slight haze to light, medium, and heavy hazeis the , the decrease of the buoyancy term in TKE is crucial, and it is mainly characterized characterised by a significant reduction of the sensible heat and the in the Q_H and MLH.

3.4.2 Critical meteorological conditions factors for the formation and dissipation of heavy air pollution

At least one previous study indicates when the MLH decreases, the concentration of atmospheric particles increases and visibility decreases (Tang et al., 2015). However, analyses of the MLH and particle concentration or visibility indicates that the correlation these is not strong (Li et al., 2015). We analysed the correlation between daily averages of MLH and visibility in this study and found that the correlation between them is poor, with a correlation coefficient of only 0.08 (Fig. 11); this finding is consistent with the results of previous study (Li et al., 2015).

Variations in the MLH represent the vertical diffusion capability of pollutants, and higher mixing layers indicate a stronger vertical diffusion capability.Variations in the wind speed represent the horizontal diffusion capability According to the discussion in Sect. 3.4.1, in addition to MLH, WS is another factor in controlling air pollution. The MLH and WS represent the vertical and horizontal diffusion capabilities of pollutants, and higher wind speeds indicate a stronger horizontal diffusion capability. In most studiesrespectively. Synthesising these two factors, the product of the MLH and the wind speed WS (ventilation coefficient: VC) is usually used as the an index to measure the capability of atmospheric diffusion; a higher VC indicates stronger capability (Tang et al., 2015). To represent the atmospheric diffusion capability during different seasons, we analysed the ventilation coefficient (VC) in the Beijing area. As shown in Fig. 11a, the atmospheric diffusion capability is the strongest Figure 12a, the VC is highest in spring with a ventilation coefficient of approximately 2000 $m^2 s^{-1}$; the atmospheric diffusion capability in summerreaches 1782, and in autumn, followed by summer, autumn, and winter, it reaches when the VC is 1782, 1095 and 1072 $m^2 s^{-1}$, respectively. The ventilation coefficient is the highest and the lowest in April and December when the maximum and minimum are 2074 and 893, respectively.

~~The ventilation coefficient in April is 2.3 times than that in December. Although~~ However, although the atmospheric diffusion capability ~~is strong in spring and summer and the atmospheric diffusion capability in summer is~~ in summer is much better than that in autumn and winter and the VC in summer can be 1.7 times ~~than that of~~ higher than in autumn and winter, the visibility is ~~the lowest (~~lowest (~ 9 km) ~~in summer~~ and the $PM_{2.5}$ concentration is ~~the~~ highest (~ 85 µg m^{-3}) in summer (Fig. ~~11a~~12a). By ~~dividing the visibility between~~focusing on visibility $\geq$ 10 km and visibility $<$ 10 km separately, we find that the ~~occurrence~~ frequency of haze ~~is highest in summer at~~ occurrence is highest (up to 73 %~~, and~~) in summer, whereas it is approximately 40 % in other seasons ~~. Therefore, the~~ (Fig. 12b). Therefore, strong diffusion capability cannot explain the occurrence of heavy pollution in summer~~and its relatively high atmospheric diffusion capability exhibit a conflicted state~~.

~~According to the discussion in Sect. 3.4.1, small differences occur in the atmospheric MLH between slight haze days and clear days. As the haze grade increases, the atmospheric MLH gradually declines, which indicates that at a slight pollutionstage,~~ To obtain a clear understanding of the relationship between the ~~degree of atmospheric pollution is essentially not related to~~ atmospheric MLH and air pollution, we analysed the correlation between daily averages of the MLH and visibility according to the RH and found that the relationship between them showed significant differences under different RH. When the RH was lower than 80 %, the correlation between the MLH and visibility was poor, but when the RH exceeded 80 %, the correlation coefficient of these two measurements significantly increased to as much as 0.72 (Fig. 11). If we assume that no transport from other regions occurs, local contributions (local emissions and secondary formation) will dominate the ~~pollution degree depends on the horizontal diffusion capability as affected by the horizontal wind speed. At the heavy pollution stage, the pollution degree is determined by the vertical diffusion capability as affected by the MLH . The statistical results of previous studies indicate that as the MLH decreases and the concentration of atmospheric particles gradually increases, the visibility gradually decreases.However, an analysis of the MLH and the~~ particle concentration~~or visibility indicates that the correlation between the MLH and the~~

particle concentration or visibility is not strong, and they may even be uncorrelated (Li ; if we further suppose that the local emission is constant every day, due to the dominant role of the aqueous, heterogeneous, and hydroscopic processes for the formation of particles in Beijing (Guo et al., 2015; Tang 2014; Sun et al., 2015). To determine the 2014), there will be little difference in the formation of particles under a fixed RH, and the column concentration in the MLH will be almost constant. Under such circumstances, the relationship between the atmospheric MLH and atmospheric pollution, we analysed the correlation between the daily average MLH and atmospheric visibility and found that the MLH and visibility should be strong. Thus, poor correlation between the MLH and atmospheric visibility is poor and has a correlation coefficient of 0.08, which is consistent with the results of previous studies (Li visibility indicates a significant influence from regional transportation, and their good correlation indicates the dominant role of local contributions. Tang et al. , (2015) . However, an analysis of the correlation between the MLH and visibility under different relative humidity showed that when the relative humidity is greater than 80, the correlation between the MLH and visibility suddenly increases and produces a correlation coefficient of 0.72 found that in light pollution, regional transport contributes heavily, whereas in heavy pollution, local contributions dominate. Because low and high RH correspond to light and heavy pollution, respectively, the two conclusions are strongly consistent.

In our data, scatters under poor relationship always corresponded to clear days and good visibility, and scatters under strong relationship corresponded to hazy days and poor visibility (Fig. 11b11). Previous studies have indicated that there are considerable differences in the chemical composition of particles between clear and haze days , and as present on clear and hazy days (Zhang et al., 2014). As the particle concentration increases, the magnitude of enhancement is highest for sulfatespercentage of sulphates, nitrates, and ammonium aerosols with relatively strong hygroscopicity strong hygroscopicity increases, whereas the magnitude of enhancement is relatively low for percentage of organic matter aerosols with relatively weak hygroscopicity . Therefore, the variation in crustal elements is not significant and exhibits higher sulfateweak hygroscopicity decreases. Thus, the aerosols exhibit higher sulphate, nitrate, and ammonium ratios on haze dayshazy days,

which indicates the dominant role of the secondary formation (Zhang et al., 2014). ~~This result also indicates that the humidity plays an important role in transforming the pollutants for heavy haze days~~

From the aforementioned analyses, the reasons for the relationships observed under conditions of low and high RH can be clearly understood. Under low ~~humidity conditions,~~ RH condition, since the significant impact of the ~~contribution of humidity-related physiochemical processes to the atmospheric particles is relatively low, and~~ regional transportation, the processes of local emissions, regional transportation, and physiochemical ~~generation~~ formation jointly dominate the concentration of atmospheric particles~~. Therefore, the correlation between visibility and the MLH is insignificant because of the contributions of particlesfrom different processes. Under high humidity conditions, the influence of regional transportation during heavy pollution periods may worsen the correlation between the heavy pollution degree and the MLH. Therefore, a relatively strong correlation indicates that heavy pollution is mainly from local contributions, which is consistent with the previous study (Tang et al., 2015). Increases in relative humidity cause~~ ; thus, the poor correlation between the MLH and visibility is occurred due to the multi-source of particles. For high RH, the RH plays an important role in transforming the trace gases to aerosols. Thus, an increase in the ~~amount of~~ RH is favourable for the formation of particles from the liquid-phase~~and heterogeneously generated chemicals and significant hygroscopic growth of particles~~, heterogeneous reactions and the hygroscopic growth processes, and the ~~main source of particle changes to locally generated~~ primary source of particles will change to local humidity-related physiochemical processes ~~.~~ during heavy pollution periods. The strong correlation of these factors under high RH indicates the dominant role of local secondary processes in heavy pollution.

Overall, the high correlation between ~~visibility and the MLH under high humidity characterizes the generation of~~ the MLH and visibility under high RH indicates that humidity-related physiochemical processes ~~as the main~~ is the primary source of atmospheric particles ~~under heavy pollution , whereas~~ in heavy pollution and that the dissipation of atmospheric particles mainly depends on the vertical diffusion capability, which is domi-

nated by the atmospheric MLH. ~~These analyses show that the primary critical condition for the formation of heavy pollution is relative humidity, and the critical threshold is~~ From the aforementioned conclusion, the MLH and RH are extracted as the key meteorological factors for the evolution of heavy air pollution, a finding that is relevant to the dissipation and formation of the atmospheric particles. Because of a sudden change of the correlation between the MLH and visibility when the RH exceeds 80 % (Tab. S1), a critical threshold of 80 % is determined for the RH. To determine the ~~other critical condition~~ critical threshold for the MLH, we analysed the fitting equation ~~during heavy haze periods when the relative humidity~~ when the RH exceeds 80 % and calculated the MLH corresponding to four different ~~degrees of pollution with atmospheric visibility of 2, 3,~~ stages with visibilities of 10, 5, ~~and 10~~3, and 2 km ~~. We~~ (Fig. 11). It is found that the ~~critical~~ threshold of MLH for the four ~~states of~~ stage are 1209, 618, 382, and 263 m, respectively. This means that when the RH is higher than 80 %, slight, light, medium, and heavy haze ~~were~~ will occur with MLH lower than 1209, 618, 382, and 263 m, respectively. ~~This result demonstrates the two critical meteorological conditions for the formation of heavy pollution and is significant for the forecasting and warning of atmospheric pollution.~~

After determining the critical meteorological ~~condition for the formation of heavy pollution, an analysis of the~~ factors for air pollution, the cause of the poor visibility in summer can be analysed according to the aforementioned conclusions. As shown in Figure 7a, summer exhibits higher RH and lower WS. The meteorological conditions in summer ~~showed that the relatively low wind speed~~ shows that low WS is a prerequisite for ~~an increase in haze days and the high relative humidity increases the generation velocity of particles~~hazy days and that high RH is conducive to the formation of particles. In addition, due to the intrusion of the west Pacific subtropical high, the frequency of cloud fraction > 50 % is the highest in summer, with greater than 70 % (Fig. ~~7a). Once the~~ 12b). When this cloud fraction increases, radiation levels will dramatically decline, and the ~~atmospheric MLH will also decrease~~ MLH will decrease significantly as well. Such conditions cause a rapid weakening of the atmospheric diffusion capability ~~and lead to the frequent occurrence of heavy pollution events with an~~ along with more rapid formation of particles under high RH; heavy

pollution will occur frequently, thus leading to the enhanced concentration of ~~atmospheric particles and reduced visibility .~~ particles and decreased visibility (Fig. 12a).

4 Conclusions

Continuous high-resolution observations of MLH are required to understand the ~~structure~~ characteristics of the atmospheric mixing layer in the Beijing and North China Plain areas. ~~In order to~~ To acquire the high-resolution observations of MLH, a study using a ceilometer was performed from July 2009 to December 2012 ~~using a ceilometer~~ in the Beijing urban area.

Based on a comparison ~~and validation of multiple types of data, we determine~~ with radiosondes, we determined that the ceilometer underestimates ~~MLH during neutral~~ the MLH during near-neutral stratification caused by strong winds ~~, whereas it overestimates~~ and that it overestimates the MLH during dust crossing. By combining ~~conventional meteorologicaldata and~~ meteorological, $PM_{2.5}$, and PM_{10} ~~observational~~ data, we ~~screen~~ screened the observation results for the MLH~~, and the~~ ; the availability of the acquired data is close to 80 %. The screened ceilometer observations are fairly consistent with the meteorological ~~radiosonde profile results. The correlation coefficient is more~~ radiosondes, with a correlation coefficient greater than 0.9~~, and the effective rate of acquired data is near 80~~. This method replaces the time-consuming method of filtering the data manually ~~, which~~ and is of great practical value for future measurements of the MLH with ceilometers.

The characteristics of ~~variation in~~ the MLH indicate that the MLH in ~~the Beijing area exhibits the feature of being~~ Beijing is low in autumn and winter, and ~~being~~ high in spring and summer. There is a significant correlation between the ~~variation in the MLH and the sensible heat flux, which characterizes~~ Q_H and MLH, which characterises the dominant role of the radiation in the ~~variations of~~ variation of the MLH. In addition, the diurnal cycle in the MLH ~~. However, the characteristics of diurnal variation in the mixing layer~~ during summer is also affected by the circulation of mountainous plain winds. The mountainous wind in summer causes a gradual decline in the mixing layer at night~~to gradually decline~~,

which suppresses ~~the development of the mixing layer~~ its development before noon, and the ~~prevalence of plain winds after noon causes the mixing layer to increase rapidly~~plain wind after noon contributes to the increase in the MLH. Therefore, compared with spring, the mountainous plain winds ~~leads to the~~ in summer lead to a concave-down ~~variation in the fast development stage~~ of the mixing layer in ~~summer compared to the spring~~the fast development stage.

By applying visibility as ~~the~~ an index for the classification of ~~atmospheric pollution degree~~ degree of air pollution, it is found that in comparison with ~~a clear day, the variation of sensible heat~~ clear days, changes in the Q_H and buoyancy term in TKE ~~of a slight haze day is insignificant , and the reduction of shear term in TKE is significant~~are insignificant on slight hazy days, but a reduction in the shear term is obvious; in comparison with ~~the slight haze day~~slight hazy days, the variation of the shear term in TKE ~~of medium and heavy haze days~~ is insignificant, ~~and the declination of sensible heat and~~ but the declines in Q_H and the buoyancy term in TKE ~~is~~ are significant. At ~~a~~ the slight pollution stage, the ~~degree of atmospheric pollution is essentially not related to the MLH and the pollution degree~~ air pollution has nothing to do with the MLH but depends on the horizontal diffusion capability as affected by the horizontal wind speed. At the heavy pollution stage, the ~~pollution degree~~ air pollution is determined by the vertical diffusion capability as affected by the MLH.

Although the correlation between the daily MLH and ~~the~~ visibility is very poor, the correlation between them is significantly enhanced ~~as the relative humidity~~ when the RH increases. The high correlation between ~~visibility and the MLH under high humidity characterizes the generation of~~ the MLH and visibility under high RH indicates that humidity-related physiochemical processes ~~as the~~ is the primary source of atmospheric particles under heavy pollution, whereas the dissipation of atmospheric particles ~~mainly depends~~ depends primarily on the vertical diffusion capability, which is dominated by the atmospheric MLH.

The aforementioned results provide reliable basic data for better portraying the structure of the boundary layer and improving the ~~parameterization scheme~~ parameterisations of the boundary layer in meteorological models. Studies ~~on~~ of the atmospheric mixing layer and its thermal dynamic ~~structure under different degrees of~~ parameters at different stages of

air pollution reveal the critical meteorological ~~conditions underlying~~ factors for the formation, evolution, and dissipation of ~~atmospheric~~ heavy pollution, ~~and provide a scientific basis~~ thus providing a useful empirical information for improving atmospheric chemistry models and the forecasting and warning of ~~atmospheric~~ air pollution.

Acknowledgements. This work was supported by ~~the~~ CAS Strategic Priority Research Program ~~Grant (no~~Grants (nos. XDB05020000 and XDA05100100)~~and~~ , the National Natural Science Foundation of China (nos. 41230642 and 41222033) ~~.~~ and the National Data Sharing Infrastructure of Earth System Science. We also gratefully acknowledge the Department of Atmospheric Science, College of Engineering, University of Wyoming for the provision of the meteorological data used in this publication.

References

Aron, R.: Mixing height – an inconsistent indicator of potential air pollution concentrations, Atmos. Environ., 17, 2193–2197, 1983.

Barbara, H. and Andrea, L.: Determination of the atmospheric boundary layer height from radiosonde and lidar backscatter, Bound.-Lay. Meteorol., 120, 181–200, 2006.

Batchvarova, E., Cai, X., Gryning, S. E., Steyn, D.: Modelling internal boundary layer development in a region with complex coastline. Bound.-Lay. Meteorol., 90, 1–20, 1999.

Baxter, R. A.: Determination of mixing heights from data collected during the 1985 SCCCAMP field program. J. Appl. Meteorol., 30, 598–606, 1991.

Beyrich, F.: Mixing height estimation from SODAR data – a critical discussion, Atmos. Environ., 31, 3941–3953, 1997.

Chen, W., Kuze, H., Uchiyama, A., Suzuki, Y., and Takeuchi, N.: One-year observation of urban mixed layer characteristics at Tsukuba, Japan using a micro pulse lidar, Atmos. Environ., 35, 4273–4280, doi:10.1016/S1352-2310(01)00181-9, 2001.

Chen, Y., Zhao, C., Zhang, Q., Deng, Z., Huang, M., and Ma, X.: Aircraft study of Mountain Chimney Effect of Beijing, China, J. Geophys. Res., 114, D08306, doi:10.1029/2008JD010610, 2009.

Chen, Z., Liu, W., Zhang, Y., He, J., and Ruan, J.: Mixing layer height and meteorological measurements in Hefei China during the total solar eclipse of 22 July, 2009, Opt. Laser Technol., 43, 50–54, doi:10.1016/j.optlastec.2010.04.022, 2011.

China Meteorological Administration (CMA): Observation and forecasting levels of haze, QX/T 113-2010, Beijing, 2010.

China Meteorological Administration (CMA): sand-dust weather almanac (2009), China Meteorological Press, Beijing, 2012.

China Meteorological Administration (CMA): sand-dust weather almanac (2010), China Meteorological Press, Beijing, 2013.

China Meteorological Administration (CMA): sand-dust weather almanac (2011), China Meteorological Press, Beijing, 2014.

China Meteorological Administration (CMA): sand-dust weather almanac (2012), China Meteorological Press, Beijing, 2015.

Coulter, R. L.: A comparison of three methods for measuring mixing layer height. J. Appl. Meteorol., 18, 1495–1499, 1979.

Devara, P. C. S., Ernest, R. P., Murthy, B. S., Pandithurai, G., Sharma, S., and Vernekar, K. G.: Intercomparison of nocturnal lower-atmospheric structure observed with LIDAR and SODAR techniques at Pune, India, J. Appl. Meteorol., 34, 1375–1383, 1995.

Ding, G. A., Chen, Z. Y., Gao, Z. Q., Yao, W. Q., Li, Y., Cheng, X. H., Meng, Z. Y., Yu, H. Q., Wong, K. H., Wang, S. F., and Miao, Q. J.: Vertical structures of PM_{10} and $PM_{2.5}$ and their dynamical character in low atmosphere in Beijing urban areas, Sci. China Ser. D, 35, 31–44, 2005.

Emeis, S. and Schäfer, K.: Remote sensing methods to investigate boundary-layer structures relevant to air pollution in cities, Bound.-Lay. Meteorol., 121, 377–385, 2006.

Emeis, S., Münkel, C., Vogt, S., Müller, W. J., and Schäfer, K.: Atmospheric boundary-layer structure from simultaneous SODAR, RASS, and ceilometer measurements, Atmos. Environ., 38, 273–286, 2004.

Emeis, S., Jahn, C., Münkel, C., Münsterer, C., and Schäfer, K.: Multiple atmospheric layering and mixing-layer height in the Inn valley observed by remote sensing, Meteorol. Z., 16, 415–424, 2007.

Emeis, S., Schäfer, K., and Münkel, C.: Surface-based remote sensing of the mixing-layer height – a review, Meteorol. Z., 17, 621–630, 2008.

Emeis, S., Schäfer, K., Münkel, C., Friedl, R., and Suppan, P.: Evaluation of the interpretation of ceilometer data with RASS and radiosonde data, Bound.-Lay. Meteorol., 143, 25–35, 2012.

Eresmaa, N., Karppinen, A., Joffre, S. M., Räsänen, J., and Talvitie, H.: Mixing height determination by ceilometer, Atmos. Chem. Phys., 6, 1485–1493, doi:10.5194/acp-6-1485-2006, 2006.

Flentje, H., Heese, B., Reichardt, J., and Thomas, W.: Aerosol profiling using the ceilometer network of the German Meteorological Service, Atmos. Meas. Tech. Discuss., 3, 3643–3673, doi:10.5194/amtd-3-3643-2010, 2010.

Garratt, J. R.: The Atmospheric Boundary Layer, Cambridge University Press, Cambridge, UK, 1992.

Guo, S.,Hu, M.,Zamora, M., Peng, J., Shang, D., Zheng, J., Du, Z., Wu, Z., Shao, M., Zeng, L., Molina, M., and Zhang, R.: Elucidating severe urban haze formation in China, 111, 17373–17378, doi:10.1073/pnas.1419604111, 2014.

Haeffelin, M., Angelini, F., Morille, Y., Martucci, G., Frey, S., Gobbi, G. P., Lolli, S., O'Dowd, C. D., Sauvage, L., Xueref-Rémy, I., Wastine, B., and Feist, D. G: Evaluation of mixing-height retrievals from automatic profiling lidars and ceilometers in view of future integrated networks in Europe, Bound.-Lay. Meteorol., 143, 49–75, 2012.

Hägeli, P., Steyn, D. G., and Strawbridge, K. B.: Spatial and temporal variability of mixed-layer depth and entrainment zone thickness, Bound.-Lay. Meteorol., 97, 47–71, 2000.

He, Q. and Mao, J.: Observation of urban mixed layer at Beijing using a micro pulse lidar, Acta Meteorol. Sin., 63, 374–384, 2005 (in Chinese).

He, Q. S., Mao, J. T., Chen, J. Y., and Hu, Y. Y.: Observational and modeling studies of urban atmospheric boundary-layer height and its evolution mechanisms, Atmos. Environ., 40, 1064–1077, doi:10.1016/j.atmosenv.2005.11.016, 2006.

Holzworth, C. G.: Estimates of mean maximum mixing depths in the contiguous United States, Mon. Weather Rev., 92, 235–242, 1964.

Holzworth, C. G.: Mixing depths, wind speeds and air pollution potential for selected locations in the United States, J. Appl. Meteorol., 6, 1039–1044, 1967.

Hu, B., Wang, Y. S. and Liu, G. R.: Relationship between net radiation and broadband solar radiation in the Tibetan Plateau. Adv. Atmos. Sci., 29(1), 135–143, doi:10.1007/s00376-011-0221-6, 2012.

Hu, X., Ma, Z., Lin, W., Zhang, H., Hu, J., Wang, Y., Xu, X., Fuentes, J. D., and Xue, M.: Impact of the Loess Plateau on the atmospheric boundary layer structure and air quality in the North China Plain: a case study, Sci. Total Environ., 499, 228–237, doi:10.1016/j.scitotenv.2014.08.053, 2014.

Hyun, Y., Kim, K., and Ha, K.: A comparison of methods to estimate the height of stable boundary layer over a temperate grassland, Agr. Forest Meteorol., 132, 132–142, doi:10.1016/j.agrformet.2005.03.010, 2005.

Kamp, D. and McKendry, I.: Diurnal and seasonal trends in convective mixed-layer heights estimated from two years of continuous ceilometer observations in Vancouver, BC, Bound.-Lay. Meteorol., 137, 459–475, 2010.

Kunz, G. J., Leeuw, G., Becker, E., and O'Dowd, C. D.: Lidar observations of atmospheric boundary layer structure and sea spray aerosol plumes generation and transport at Mace Head, Ireland (PARFORCE experiment), J. Geophys. Res., 107, 8106, doi:10.1029/2001JD001240, 2002.

Li, M., Tang, G., Huang, J., Liu, Z., An, J., and Wang, Y.: Characteristics of winter atmospheric mixing layer height in Beijing-Tianjin-Hebei region and their relationship with the atmospheric pollution, Environ. Sci., 36, 1935–1943, 2015 (in Chinese).

Liu, Z, Hu, B., Wang, L., Wu, F., Gao, W., and Wang, Y.: Seasonal and diurnal variation in particulate matter (PM_{10} and $PM_{2.5}$) at an urban site of Beijing: analyses from a 9-year study, Environ. Sci. Pollut. R., 22, 627–642, ~~2015.~~ 2014.

Luo, T., Yuan, R., and Wang, Z.: Lidar-based remote sensing of atmospheric boundary layer height over land and ocean, Atmos. Meas. Tech., 7, 173–182, doi:10.5194/amt-7-173-2014, 2014.

McKendry, I. G., Kamp, D., Strawbridge, K. B., Christen, A., and Crawford, B.: Simultaneous observations of boundary-layer aerosol layers with CL31 ceilometer and 1064/532 nm lidar, Atmos. Environ., 43, 5847–5852, doi:10.1016/j.atmosenv.2009.07.063, 2009.

Münkel, C. and Räsänen, J.: New optical concept for commercial lidar ceilometers scanning the boundary layer, P. SPIE, 5571, 364–374, 2004.

Münkel, C., Eresmaa, N., Räsänen, J., and Karppinene, A.: Retrieval of mixing height and dust concentration with lidar ceilometer, Bound.-Lay. Meteorol., 124, 117–128, 2007.

Muňoz, R. C. and Undurraga, A. A.: Daytime mixed layer over the Santiago Basin: Description of two years of observations with a lidar ceilometer, J. Appl. Meteorol. Clim., 49, 1728–1741, 2010.

Pappalardo, G., Amodeo, A., Apituley, A., Comeron, A., Freudenthaler, V., Linné, H., Ansmann, A., Bösenberg, J., D'Amico, G., Mattis, I., Mona, L., Wandinger, U., Amiridis, V., Alados-Arboledas, L., Nicolae, D., and Wiegner, M.: EARLINET: towards an advanced sustainable European aerosol lidar network, Atmos. Meas. Tech., 7, 2389-2409, doi:10.5194/amt-7-2389-2014, 2014.

Quan, J., Gao, Y., Zhang, Q., Tie, X., Cao, J., Han, S., Meng, J., Chen, P., and Zhao, D.: Evolution of planetary boundary layer under different weather conditions, and its impact on aerosol concentrations, Particuology, 11, 34–40, doi:10.1016/j.partic.2012.04.005, 2013.

Russell, P. B., Uthe, E. E., Ludwig, F. L., Shaw, N. A.: A comparison of atmospheric structure as observed with monostatic acoustic sounder and lidar techniques. J. Geophys. Res., 79, 5555–5566, 1974.

Scarino, A. J., Obland, M. D., Fast, J. D., Burton, S. P., Ferrare, R. A., Hostetler, C. A., Berg, L. K., Lefer, B., Haman, C., Hair, J. W., Rogers, R. R., Butler, C., Cook, A. L., and Harper, D. B.: Comparison of mixed layer heights from airborne high spectral resolution lidar, ground-based measurements, and the WRF-Chem model during CalNex and CARES, Atmos. Chem. Phys., 14, 5547–5560, doi:10.5194/acp-14-5547-2014, 2014.

Schäfer, K., Emeis, S., Hoffmann, H., and Jahn, C.: Influence of mixing layer height upon air pollution in urban and sub-urban area, Meteorol. Z., 15, 647–658, doi:10.1127/0941-2948/2006/0164, 2006.

Schneider, J. and Eixmann, R.: Three years of routine Raman lidar measurements of tropospheric aerosols: Backscattering, extinction, and residual layer height, Atmos. Chem. Phys., 2, 313–323, doi:10.5194/acp-2-313-2002, 2002.

Schween, J. H., Hirsikko, A., Löhnert, U., and Crewell, S.: Mixing-layer height retrieval with ceilometer and Doppler lidar: from case studies to long-term assessment, Atmos. Meas. Tech., 7, 3685–3704, doi:10.5194/amt-7-3685-2014, 2014.

Seibert, P., Beyrich, F., Gryning, S.-E., Joffre, S., Rasmussen, A., and Tercier, P.: Review and intercomparison of operational methods for the determination of the mixing height, Atmos. Environ., 34, 1001–1027, 2000.

Sicard, M., Pérez, C., Rocadenbosch, F., Baldasano, J. M., and Garcia-Vizcaino, D.: Mixed-Layer depth determination in the Barcelona coastal area from regular lidar measurements: Methods, results and limitations, Bound.-Lay. Meteorol., 119, 135–157, 2006.

Sicard, M., D'Amico, G., Comerón, A., Mona, L., Alados-Arboledas, L., Amodeo, A., Baars, H., Baldasano, J. M., Belegante, L., Binietoglou, I., Bravo-Aranda, J. A., Fernández, A. J., Fréville, P., García-Vizcaíno, D., Giunta, A., Granados-Muñoz, M. J., Guerrero-Rascado, J. L., Hadjimitsis, D., Haefele, A., Hervo, M., Iarlori, M., Kokkalis, P., Lange, D., Mamouri, R. E., Mattis, I., Molero, F., Montoux, N., Muñoz, A., Muñoz Porcar, C., Navas-Guzmán, F., Nicolae, D., Nisantzi, A., Papagiannopoulos, N., Papayannis, A., Pereira, S., Preißler, J., Pujadas, M., Rizi, V., Rocadenbosch, F., Sellegri, K., Simeonov, V., Tsaknakis, G., Wagner, F., and Pappalardo, G.: EARLINET: potential operationality of a research network, Atmos. Meas. Tech., 8, 4587-4613, doi:10.5194/amt-8-4587-2015, 2015.

Song, T. and Wang, Y.: Carbon dioxide fluxes from an urban area in Beijing, Atmos. Res., 106, 139–149, doi:10.1016/j.atmosres.2011.12.001, 2012.

Song, T., Sun, Y., and Wang, Y.: Multilevel measurements of fluxes and turbulence over an urban landscape in Beijing, Tellus B, 65, 20421, doi:10.3402/tellusb.v65i0.20421, 2013.

Steyn, D. G., Baldi, M., and Hoff, R. M.: The detection of mixed layer depth and entrainment zone thickness from lidar backscatter profiles, J. Atmos. Ocean. Tech., 16, 953–959, 1999.

Strawbridge, K. B. and Snyder, B. J.: Planetary boundary layer height determination during Pacific 2001 using the advantage of a scanning lidar instrument, Atmos. Environ., 38, 5861–5871, doi:10.1016/j.atmosenv.2003.10.065, 2004.

Stull, R. B.: An Introduction to Boundary Layer Meteorology, Kluwer Academic Publishers, Dordrecht, 1988.

Sun, Y., Wang, Z., Fu, P., Jiang, Q.,Yang, T., Li, J., and Ge, X.: The impact of relative humidity on aerosol composition and evolution processes during wintertime in Beijing, China, Atmos. Environ., 77, 927–934, doi:10.1016/j.atmosenv.2013.06.019, 2013.

Tang, G., Li, X., Wang, Y., Xin, J., and Ren, X.: Surface ozone trend details and interpretations in Beijing, 2001–2006, Atmos. Chem. Phys., 9, 8813–8823, doi:10.5194/acp-9-8813-2009, 2009.

Tang, G., Wang, Y., Li, X., Ji, D., Hsu, S., and Gao, X.: Spatial-temporal variations in surface ozone in Northern China as observed during 2009–2010 and possible implications for future air quality control strategies, Atmos. Chem. Phys., 12, 2757–2776, doi:10.5194/acp-12-2757-2012, 2012.

Tang, G., Zhu, X., Hu, B., Xin, J., Wang, L., Münkel, C., Mao, G., and Wang, Y.: ~~Vertical variations of aerosols and the effects responded to the emission control: application of lidar ceilometer~~ Impact of emission controls on air quality in Beijing during APEC ~~,~~2014: lidar ceilometer observations, Atmos. Chem. Phys.~~Discuss.~~, 15, ~~13173–13209~~12667–12680, doi:10.5194/acp-15-12667-2015, 2015.

Vogelezang, D. H. P. and Holtslag, A. A. M.: Evolution and model impacts of alternative boundary layer formulations, Bound.-Lay. Meteorol., 81, 245–269, 1996.

Wang, X. Y. and Wang, K. C.: Estimation of atmospheric mixing layer height from radiosonde data, Atmos. Meas. Tech., 7, 1701–1709, doi:10.5194/amt-7-1701-2014, ~~2014.~~ 2014a.

Wang, Y. H., Hu, B., Ji, D. S., Liu, Z. R., Tang, G. Q., Xin, J. Y., Zhang, H. X., Song, T., Wang, L. L., Gao, W. K., Wang, X. K., and Wang, Y. S.: Ozone weekend effects in the Beijing-Tianjin-Hebei metropolitan area, China, Atmos. Chem. Phys., 14, 2419–2429, doi:10.5194/acp-14-2419-2014, 2014b.

Wang, Z., Cao, X., Zhang, L., Notholt, J., Zhou, B., Liu, R., and Zhang, B.: Lidar measurement of planetary boundary layer height and comparison with microwave profiling radiometer observation, Atmos. Meas. Tech., 5, 1965–1972, doi:10.5194/amt-5-1965-2012, 2012.

White, A. B., Senff, C. J., and Banta, R. M.: A Comparison of mixing depths observed by ground-based wind profilers and an airborne lidar, J. Atmos. Ocean. Tech., 16, 584–590, 1999.

Wiegner, M., Emeis, S., Freudenthaler, V., Heese, B., Junkermann, W., Münkel, C., Schäfer, K., Seefeldner, M., and Vogt, S.: Mixing layer height over Munich, Germany: variability and comparisons of different methodologies, J. Geophys. Res., 111, D13201, doi:10.1029/2005JD006593, 2006.

Wiegner, M.,Madonna, F, Binietoglou, I., Forkel, R., Gasteiger, J., Geiß, A., Pappalardo, G., Schäfer, K., and Thomas, W.: What is the benefit of ceilometers for aerosol remote sensing? An answer from EARLINET, Atmos. Meas. Tech., 7, 1979–1997, doi:10.5194/amt-7-1979-2014, 2014.

Xin, J., Wang, Y., Tang, G., Wang, L., Sun, Y., Wang, Y. H., Hu, B., Song, T., Ji, D. S., Wang, W. F., Li, L., and Liu, G. R.: Variability and reduction of atmospheric pollutants in Beijing and its surrounding area during the Beijing 2008 Olympic Games, Chinese Sci. Bull., 55, 1937–1944, 2010.

Yang, D. W., Li, C., Lau, A. K.-H., and Li, Y. Long-term measurement of daytime atmospheric mixing layer height over Hong Kong, J. Geophys. Res., 118, 2422–2433, 2013.

Yang, H., Liu, W., Lu, Y., Xie, P., Xu, L., Zhao, X., Yu, T., and Yu, J.: PBL observations by lidar at Peking, Optical Tech., 31, 221–226, 2005.

Yang, Y. R., Liu, X. G., Qu, Y., An, J. L., Jiang, R., Zhang, Y. H., Sun, Y. L., Wu, Z. J., Zhang, F., Xu, W. Q., and Ma, Q. X.: Characteristics and formation mechanism of continuous hazes in China: a case study during the autumn of 2014 in the North China Plain, Atmos. Chem. Phys., 15, 8165–8178, doi:10.5194/acp-15-8165-2015, 2015.

Ye, X., Wu, B., and Zhang, H.: The turbulent structure and transport in fog layers observed over the Tianjin area, Atmos. Res., 153, 217–234, doi:10.1016/j.atmosres.2014.08.003, 2015.

Zhang, J. K., Sun, Y., Liu, Z. R., Ji, D. S., Hu, B., Liu, Q., and Wang, Y. S.: Characterization of submicron aerosols during a month of serious pollution in Beijing, 2013, Atmos. Chem. Phys., 14, 2887–2903, doi:10.5194/acp-14-2887-2014, 2014.

Zhang, Q., Quan, J., Tie, X., Li, X., Liu, Q., Gao, Y., and Zhao, D.: Effects of meteorology and secondary particle formation on visibility during heavy haze events in Beijing, China, Sci. Total Environ., 502, 578–584, doi:10.1016/j.scitotenv.2014.09.079, 2015.

Zhang, X., Cai, X., and Chai, F.: Structures and characteristics of the atmospheric boundary layer over Beijing area in autumn, Acta Sci. Natur. Univ. Pekinensis, 42, 220–225, 2006 (in Chinese).

Zilitinkevich, S. and Baklanov, A.: Calculation of the height of the stable boundary layer in practical applications, Bound.-Lay. Meteorol., 105, 389–409, 2002.

Table 1. Site description and instrument list. BJT refers to the Beijing tower; ZBAA is the international standard weather station.

Sites	Long, lat	Instruments	Time interval	Time resoluti
BJT	~~116.37, 39.97~~116.372, 39.974	CL31	15 Jul ~~2009–31~~ 2009–16 Dec 2012	10 min
		$PM_{2.5}$,PM_{10}	15 Jul 2009–31 Dec 2012	60 min
		Tower-based meteorology	15 Jul 2009–31 Dec 2012	~~5~~30 min
ZBAA	~~116.28, 39.48~~116.282, 39.484	Weather balloons	15 Jul 2009–31 Dec 2012	1 per week a
		Weather balloons	1 Jan 2012–31 Dec 2012	08:00 and 20
		Ground-based meteorology	15 Jul 2009–31 Dec 2012	30 min

Discussion Paper | Discussion Paper | Discussion Paper | Discussion Paper |

Table 2. Statistics of the thermal/dynamic parameters according to visibility.

Parameters	Clear days Vis $\geq$ 10 km	Slight haze 5 km $\leq$ Vis $<$ 10 km	Light haze 3 km $\leq$ Vis $<$ 5 km	Medium haze 2 km $\leq$ Vis $<$ 3 km	Heavy haze Vis $<$ 2 km
WS ($m\,s^{-1}$)	3.8	2.5	2.1	2.0	1.8
RH (%)	43.3	63.1	73.4	79.6	86.4
MLH (m)	664	671	586	430	320
Q^* ($W\,m^{-2}$)	77.6	74.6	63.9	53.6	32.8
Q_H ($W\,m^{-2}$)	20.4	19.7	15.2	12.8	7.8
Q_E ($W\,m^{-2}$)	18.7	19.9	21.5	18.8	19.8
u_* ($m\,s^{-1}$)	0.45	0.32	0.28	0.26	0.23
$\overline{e}$ ($m^2\,s^{-2}$)	0.99	0.64	0.56	0.52	0.46
BT ($\times\ 10^{-3}\,m^2\,s^{-3}$)	0.67	0.64	0.49	0.39	0.24
ST ($\times\ 10^{-3}\,m^2\,s^{-3}$)	1.02	0.66	0.37	0.26	0.23

WS: wind speed; RH: relative humidity; Q^*: net radiation; Q_H: sensible heat; Q_E: latent heat; u_*: friction velocity; $\overline{e}$: TKE per unit mass; BT: buoyancy term in TKE; ST: shear term in TKE.

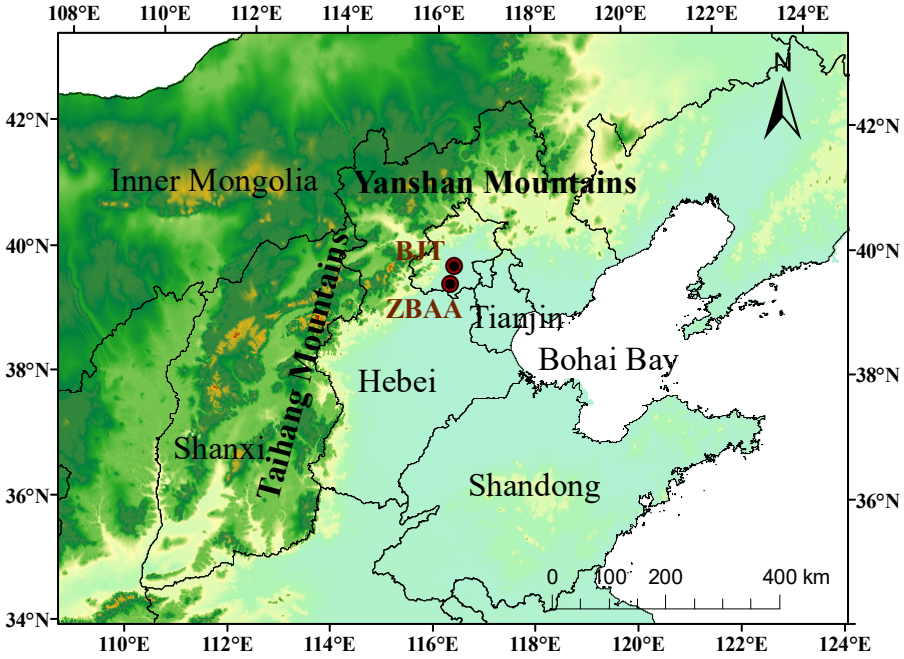

Figure 1. Topography and the observation sites.

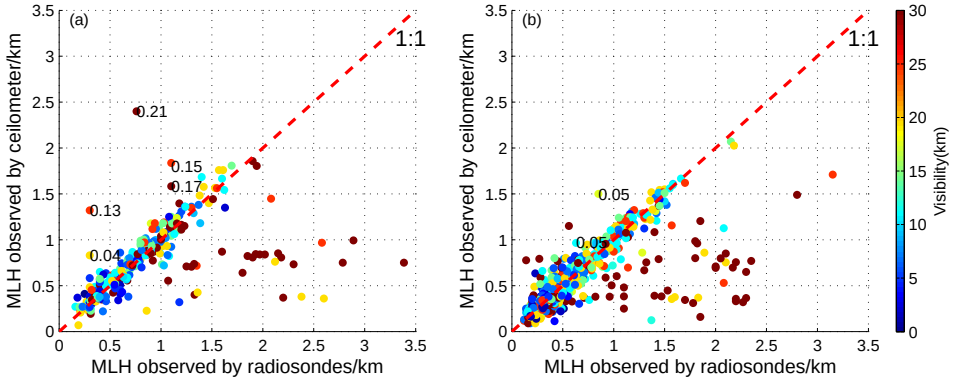

Figure 2. ~~The comparison~~ Comparison of MLH between radiosondes and the ceilometer according to visibility for convective **(a)** and stable **(b)** states, the number refers to the ratios of $PM_{2.5}$ and PM_{10} when sand-dust is crossing.

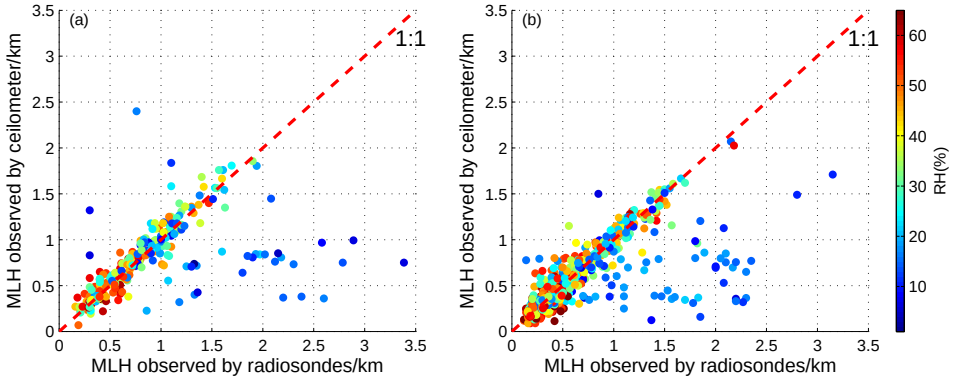

Figure 3. ~~The comparison~~ Comparison of MLH between radiosondes and the ceilometer according to ~~humidity~~ RH for convective **(a)** and stable **(b)** states.

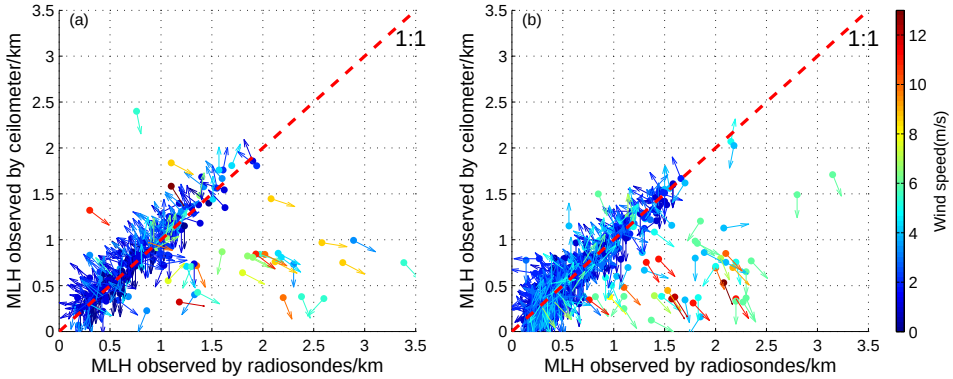

Figure 4. ~~The comparison~~ Comparison of MLH between radiosondes and the ceilometer according to ~~vector winds~~ wind vectors for convective **(a)** and stable **(b)** states.

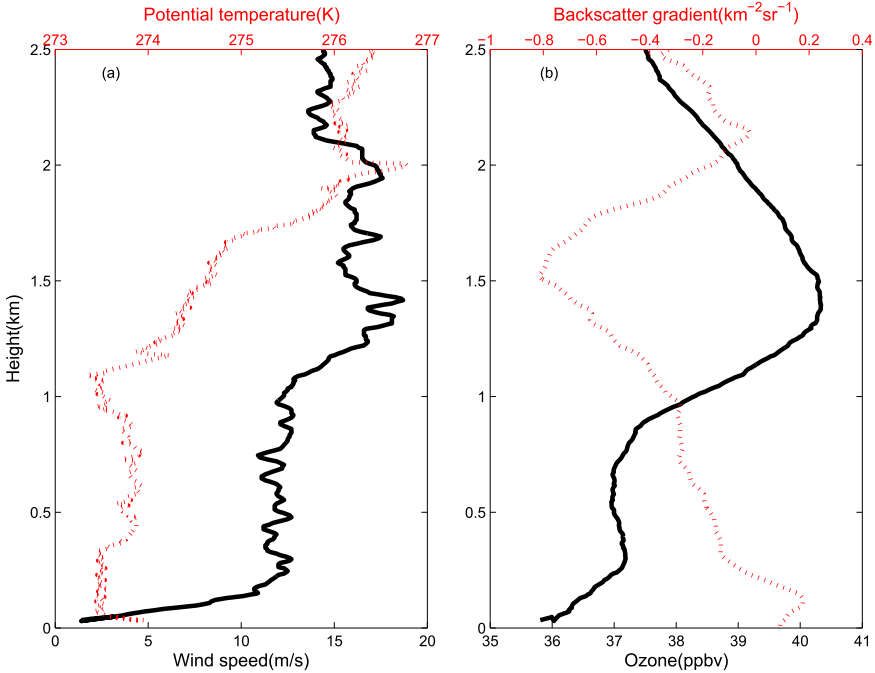

Figure 5. ~~The virtual~~ Virtual potential temperature and wind speed **(a)**, and ozone and backscatter gradients **(b)** at 14:00 LT on 29 December 2009 in Beijing.

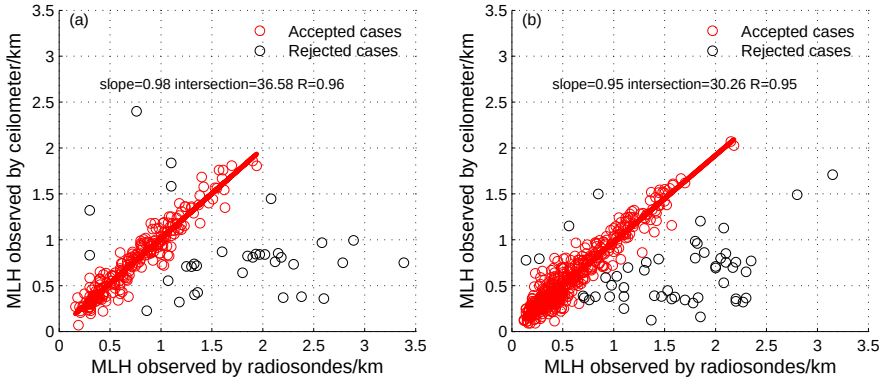

Figure 6. ~~The comparison~~ Comparison of MLH between the ceilometer and radiosondes for convective **(a)** and stable **(b)** states.

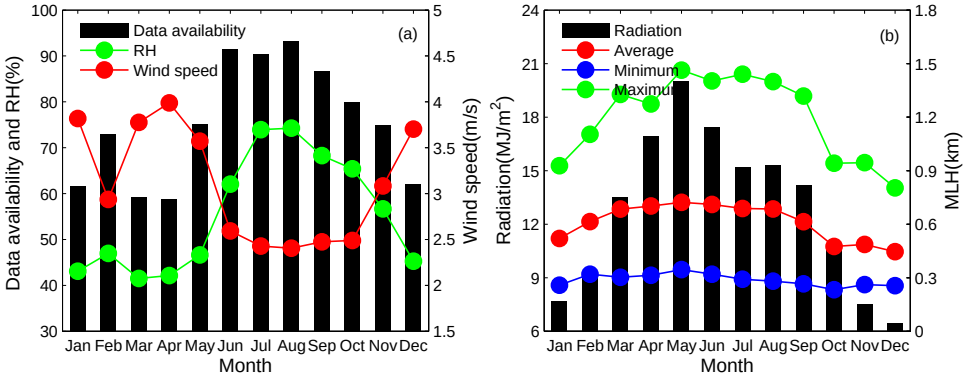

Figure 7. Monthly variations in the effective rate, wind speed, and ~~relative humidity (~~RH ~~)~~ **(a)**, and MLH and total radiation flux **(b)** in Beijing.

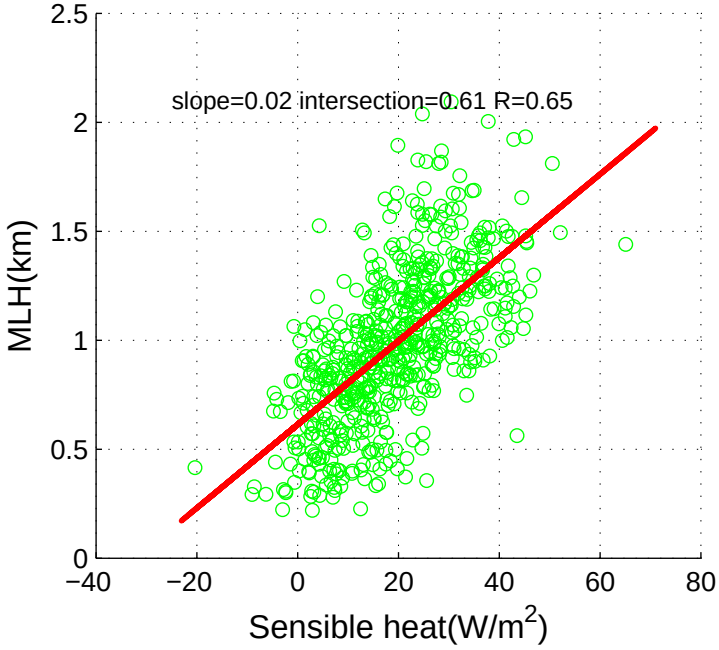

Figure 8. ~~The correlation~~ Correlation between ~~the~~ sensible heat and MLH in Beijing.

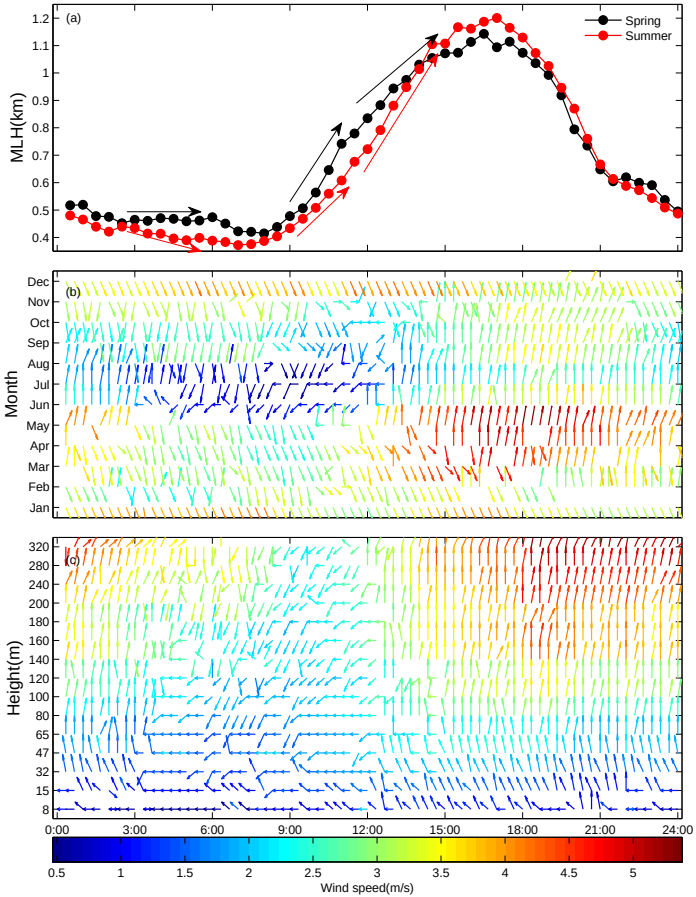

Figure 9. ~~The daily~~ Daily variations in MLH in spring and summer **(a)**, seasonal wind vectors at 100 m **(b)**, and vertical profiles of wind vectors in July **(c)** in Beijing.

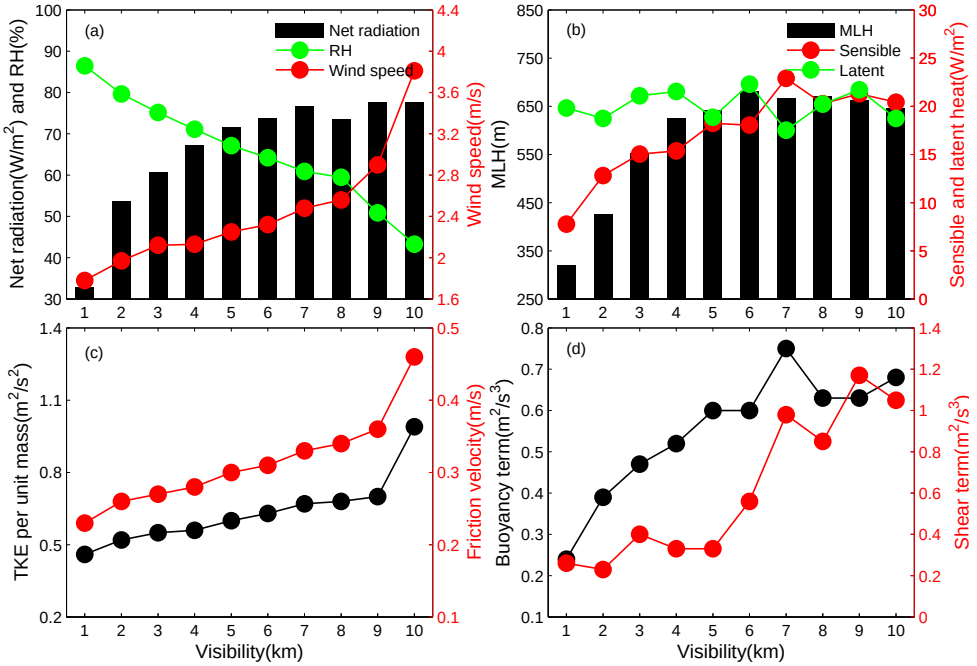

Figure 10. ~~The variations~~ Variations in net radiation, ~~relative humidity (~~RH~~)~~, and wind speed **(a)**, MLH, sensible and latent heat **(b)**, TKE per unit mass, and ~~fraction~~ friction velocity **(c)**, and buoyancy and shear term in TKE **(d)** according to ~~different~~ visibility~~levels~~.

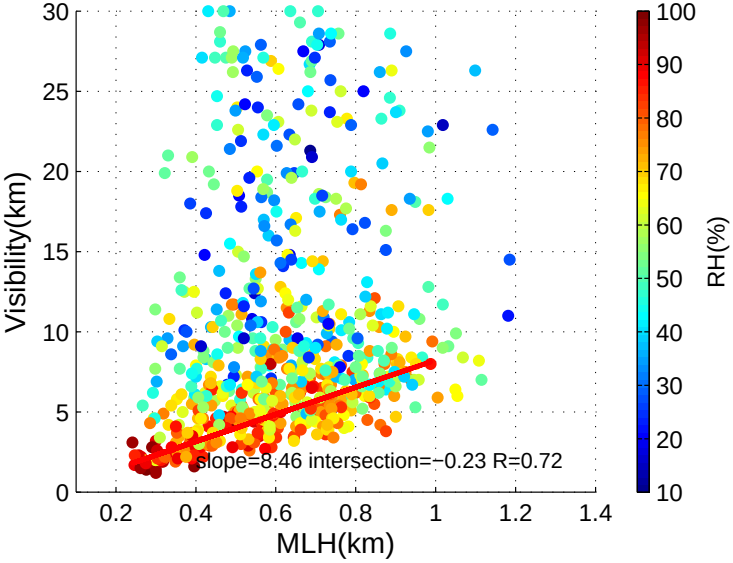

Figure 11. ~~Monthly variations in visibility and ventilation coefficients **(a)** and the correlation~~ Correlation between the MLH and visibility according to ~~the relative humidity (~~RH ~~) **(b)**~~ in Beijing.

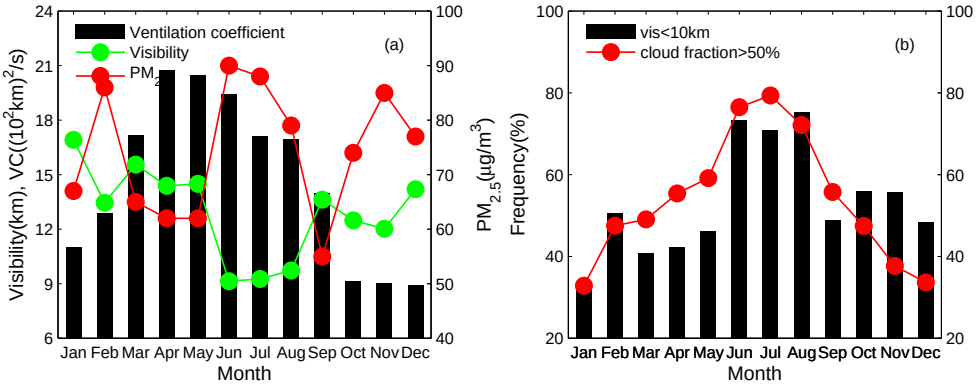

Figure 12. Monthly variations in visibility, $PM_{2.5}$, and ventilation coefficients **(a)** and frequency of visibility < 10 km, and cloud fraction > 50 % **(b)** in Beijing.

Response to comments by referee 1

We would like to thank you for your comments and helpful suggestions. We revised our manuscript according to these comments and suggestions.

Specific comments:
The paper deals with the determination of the MLH over Beijing during more than 3 years from ceilometer measurements and its correlation with pollution classes (clear days, slight, light, medium and heavy haze). Most of the paper is devoted to a meteorologically based discussion why the correlations are as they are. This is certainly a positive feature of the paper as often just statements are given without any critical scrutiny. The authors consider a variety of parameters derived from different measurements (e.g., meteorological tower), so the discussion is quite elaborated. However, the readability is often very difficult because a separation of very long sections into different paragraphs is missing, information is only put into words where a table would be helpful, and often it is difficult to follow because the expressions are not clear but unnecessarily complex or in bad English. Consequently, it is sometimes hard to check the validity of the authors' conclusions.
Thus, I strongly recommend to make the text more concise, to clarify statements, to delete redundancies and to improve its consistency. And ask a native speaker or a professional office for improving the language. If this is provided (implying major revisions) the paper can be foreseen for publication. A few suggestions and technical comments (in chronological order, not ordered in terms of importance) for improvements are made below, but it is not possible to review/amend every single expression or sentence.

Responses：
Thank you for your kindly comments and suggestions. We are sorry for the bad presentation in our manuscript. In the revised version of our manuscript, several long paragraphs were separated into some small parts or rephrased concisely. We deleted some redundancies and adjusted the sequences of the sentences to make the manuscript more fluent. Afterwards, a native speaker polished our manuscript to make the language better for the reader.

Specific comments：
Question 1
(28251,7):
"The height to which the atmospheric mixing layer extends is the mixing layer height (MLH)". This sentence is more or less trivial and does not help to explain
Response 1
Thank you for your suggestions. We have deleted this sentence.

Question 2
• (28251,11):

"gradients" →"concentration"
Response 2
Thank you for your suggestions. We have fixed it.

Question 3
• (28251,22):
"1000 m": is this really true, this value seems to be extremely large
Response 3
Thank you for your suggestion. We are sorry for the misunderstanding. We have deleted “to 1000m” in the revised manuscript.

Question 4
• (28251,23):
"...even the hourly observations...": which data set is meant here? Or should it be something like "even if hourly observations would be available they would not provide a sufficient temporal resolution"? Please clarify.
Response 4
Thank you for your suggestion. We have revised it as follows.
When solar radiation increases in the morning, the growth rate of the MLH reaches hundreds of metres per hour and convection develops quickly; even if hourly observations were available, they could not provide sufficient temporal resolution of MLH evolution (Seibert et al., 2000).

Question 5
• (28251,24):
I would not mention airborne measurements because they cannot provide routine measurements. They can only be used for case studies.
Response 5
Thank you for your suggestion. Absolutely airborne measurement is not a routine measurement for the mixing layer height. However, as for the introduction, I think we should show the reader all the measurements to observe the mixing layer height.

Question 6
(28252,4):
"light intensity detection and ranging": delete "intensity"
Response 6
Thank you for your suggestion. We have deleted all the acronyms because the names of the measurements are well known.

Question 7
• (28252,5):
for consistency reasons replace "Doppler radar" by "radar" and explain the acronym. Or do not explain all acronyms (sodar, lidar and radar are well known)!
Response 7

Thank you for your suggestion. We have deleted all the acronyms because the names of the measurements are well known.

Question 8
• (28252,7):
delete "variations in"
Response 8
Thank you for your suggestion. We have fixed it.

Question 9
• (28252,14):
"visible light band": many lidars operate in the UV and NIR, i.e. not visible.
Response 9
Thank you for your suggestion. We have deleted this sentence.

Question 10
• (28252, 17):
"Wind radar is easily interfered by clouds, and the observational height is limited under cloudy conditions." This sentence does not fit here (previous and next sentence is on lidar). By the way: the lidar range is also limited in the presence of clouds.
Response 10
Thank you for your suggestion. We have adjusted the sequence of the sentences. By the way, we have revised the sentence about the wind rader as follows.
The lowest detection height of wind radar is normally above 200 m, and the vertical resolution is limited to 50-250 m, factors that make the interpretation of wind radar data not always straightforward (Seibert et al., 2000).

Question 11
• (28252,24):
"...the eye-safe ceilometers..." This is a feature of all ceilometers, not only of Vaisala-ceilometers. This sentence must be more general, you can cite the AMT paper (Earlinet special issue) on the benefit of ceilometers.
Rersponse 11
Thank you for your suggestion. We have deleted “Vaisala”. We really thank you for your suggestion of the AMT paper, and we have read these carefully and added some references here and elsewhere.

Question 12
• (28253,11):
"...and the atmospheric stratification is stable..." Is this in contrast to the findings on (28255,24) where the authors find "only" 540 out of 800 cases to be stable?
Response 12
Because we acquired a lot of data during 8:00 and 20:00 LT but less data during 14:00 LT, the number of samples in stable condition is much more than that in convective

conditions. In this section, the atmospheric stratification is stable during heavy pollution episodes. In order to clarify this sentence, we have revised as follows.
Previous studies of Beijing have indicated that visibility declines dramatically when the concentration of particles increases; the weather conditions typically include high relative humidity (RH), stable atmospheric stratification, and low wind speed (WS) with a southern flow (Ding et al., 2005; Liu et al., 2014; Zhang et al., 2015).

Question 13
(28253,22):
The citations "He and Mao, 2005; Yang et al., 2005;..." should be moved to line 20: after "during heavy pollution periods". At the present position it might be confusing.
Response 13
Thank you for your suggestion. We have fixed it.

Response 14
• (28254,1):
"variation characteristics" → "temporal development"
Response 14
Thank you for your suggestion. We have fixed it.

Question 15
• (28254,1):
"3 years"? In the previous sentence it was "3 years and 5 months" (whereas "July of 2009 to December of 2012" is 3 years and 6 months)
Response 15
Exactly, the observation started from 15th July 2009 and ended on 16th December 2012. If we calculated the observation period using the number of days, it should be 3 years and 5 months. However, we think you are right. We should use 3 years and 6 months in order to eliminate the misunderstanding.

Question 16
• (28254,19):
39.97: Give all geographical coordinates with 3 or 4 decimal places
Response 16
Thank you for your suggestion. We have fixed it.

Question 17
• (28254,22):
"...attenuated backscatter coefficient profile of atmospheric aerosols..." This is not exactly true as water vapor absorption occurs (there are similar expressions elsewhere in the paper).
Response 17
Thank you for your suggestion. The attenuated backscattering coefficient is not the

same as aerosol concentrations, which is influenced by the water vapor absorption (Wiegner et al., 2014). Therefore, we have revised this mistake in proper words in the manuscript according to your suggestions. The revisions mainly include removing the word “aerosol” and adding some descriptions about the observed deviations due to water vapor absorption.

Question 18
• (28255,5):
How is radiation measured by "ultrasonic anemometers"? Use clear descriptions!
Response 18
I am sorry for our mistakes. I have added some sentences to clarify the mistakes. Please see as follows.
The thermodynamic parameters (sensible heat, latent heat, friction velocity, etc.) and the total (285-2800 nm) and net (0.2-100 μm) radiation during the same period were observed using ultrasonic anemometers (CSAT3, Campbell Scientific, USA), a pyranometer (CM11, Kipp & Zonen, Netherlands) and a net radiometer (NR Lite2, Kipp & Zonen), respectively. All of these data were obtained on the meteorological tower at a height of 280 m and processed with a resolution of 30 min. A detailed description is provided by Hu et al. (2012) and Song and Wang (2012).

Question 19
• (28255,8):
PM2.5 and PM10 were measured at the ground?
Response 19
Yes, the observations of particles were setup on the ground. We have added some descriptions about the observations as follows.
To identify the sand-dust crossing, the ratio of $PM_{2.5}$ and PM_{10} was used as an index. If there was no sand-dust crossing, the ratio of $PM_{2.5}$ to PM_{10} might almost exceed 50% (Liu et al., 2014). A sudden decrease in the ratio to 30 % or lower and PM_{10} concentration higher than 500 μg m^{-3} usually indicate a sand-dust crossing. The ground observations of $PM_{2.5}$ and PM_{10} during the same period were made by the ambient particulate monitor (RP1400a, Thermo Fisher Scientific, USA). The data were acquired at a time resolution of 5 min and processed with a resolution of 60 min. A detailed description is provided by Liu et al. (2014).

Question 20
• (28255,26):
"...visibility at station..." How is this measured? How accurate are these numbers? It would help to have this information as it is of importance for subsequent sections of the paper.
Response 20
Thank you for your suggestion. The visibility was measured in ZBAA site using the

visibility sensor (PWD12, Vaisala, Finland) with an accuracy of ±10%.

Question 21
(28255,27):
"...of Wyoming Engineering University (http://weather.uwyo.edu)." Give a more precise URL and name of the institution. Maybe it can be added to the acknowledgements.
Response 21
Thank you for your suggestion. We have revised as follows.
Visibility at station ZBAA, which was obtained from the Department of Atmospheric Science, College of Engineering, University of Wyoming (http://weather.uwyo.edu/surface/meteorogram/), was measured by a visibility sensor (PWD12, Vaisala, Finland) with an accuracy of ±10%.

Question 22
• (28256,3):
"is relatively long and" can be deleted.
Response 22
Thank you for your suggestion. We have fixed it.

Question 23
• (28256,7):
"...backscatter coefficient profile of atmospheric particles". delete: "of atmospheric particles"
Response 23
Thank you for your suggestion. We have fixed it.

Question 24
• (28256,9):
"...we use the gradient method": It should be outlined whether the Vaisala firmware is used or own retrievals have been developed. Especially in the latter case the retrieval should be explained in 2–3 sentences. What is the lowermost level, where the MLH can be detected? Is an overlap correction applied?
Response 24
Thank you for your suggestion. We have added some explanations according to your suggestion as follows.
Time averaging is dependent on the current signal noise; the intervals vary from 14 to 52 min for the CL31. Height averaging intervals range from 80 m at ground level to 360 m at 1600 m height and beyond. Additional features of this algorithm, which is used in the Vaisala software product BL-VIEW, are cloud and precipitation filtering and outlier removal.

Question 25
• (28256,13):

"...spatial and temporal averaging...": give typical values.
Response 25
Thank you for your suggestion. We have revised it, please see the response 24.

Question 26
• (28256,19):
"convective state": delete "state"
Response 26
Thank you for your suggestion. We have fixed it.

Question 27
• (28256,21):
"variations" → "profiles"
Response 27
Thank you for your suggestion. We have fixed it.

Question 28
• (28257,8):
"and the results were evaluated." I believe that can be deleted too.
Response 28
Thank you for your suggestion. We have fixed it.

Question 29
(28257,11):
delete "of atmospheric particles"
Response 29
Thank you for your suggestion. We have fixed it.

Question 30
• (28257,3): Section 3.1
If a "verification" shall be provided it must be defined what is considered as "truth". It seems that the radio soundings are used as reference. This should be clearly stated. Another important aspect is that it is not clear what the "error" of the ceilometer data is (backscatter profile? MLH-determination?, relative error? Absolute error?...). This must be clarified at different places of the manuscript.
Response 30
Thank you for your suggestion. We used radiosondes as reference as you said. The error introduced in the manuscript is absolute error, and we have clarified it in the revised manuscript. We have revised the manuscript according to your suggestion as follows.
Previous studies with ceilometers did not resolve issues concerning the applicability of ceilometers in Chinese areas with high aerosol concentrations. According to the methods described in Sect. 2.1.2, 260 and 540 effective observation samples were obtained for the stable and convective states,

respectively. The MLH data acquired by meteorological radiosondes and by ceilometer were compared for the two types of weather conditions (Fig. 2). Using the MLH calculated from the radiosondes as a reference, the results showed that the MLH observed by the ceilometer was overestimated or underestimated in a portion of the samples.

Question 31
• (28257,10):
The whole sentence starting with "Because the ceilometer determines..." is not clear. What is the measurement error? How is it determined? This has to be explained in Section 2.2.1. Give a reason why the error increases when the concentration is low?
Response 31
Thank you for your suggestion. We have revised it as follows.
Because the ceilometer determines the MLH by measuring the attenuated backscatter profile, if the concentration of atmospheric particles is relatively low, it will be difficult to determine the MLH based on a sudden change in the backscatter profile, and use of this method will lead to a higher absolute error (AE) of the measured MLH (Eresmaa et al., 2006; Munoz and Undurraga, 2010). When taking the visibility into account, we found that the underestimations of the observed MLH always occurred when visibility was good. However, there were still a number of samples that had low AE under conditions of good visibility (Fig. 2). Consequently, clear days with good visibility are not the main reason for underestimation of the observed MLH.

Question 32
• (28257,14):
"An analysis...". The sentence is not clear at all, must be re-phrased. If "visibility" is introduced here: where does this information comes from? What is "high" and "low" visibility? How is it measured? What is its accuracy?
Response 32
Thank you for your suggestion. We have rephrased this paragraph. Please refer to response 31.
As for the visibility, please see the response 20.

Question 33
• (28257,19):
"...predict underestimations". See remark to (28257,3). What is the reference?
Response 33
Thank you for your suggestion. We have rephrased this paragraph, please see the response 31.

Question 34
• (28257,22):
A bi-level structure (two layers are meant?) could be better seen if the attenuated

backscatter profile is added to Fig. 2b.
Response 34
Thank you for your suggestion. A bi-level structure is meant two layers, but the two layers structure can only be observed by the radiosondes. We cannot acquire the two layers structure because of the sand-dust crossing. This is the main reason that the overestimations of the MLH during sand-dust crossing. In order to clarify this question, we used the calculated backscatter gradients to explain this overestimation, and rewrite this paragraph as follows.
With respect to overestimations of the ceilometer results, we may take the meteorological radiosonde at 14:00 LT on 29 December 2009 as an example (Fig. 5). The MLH is determined at approximately 1100 m, where the virtual potential temperature and the WS begin to increase; the ozone concentration is transported from the background area, where ozone is present at approximately 40 ppbv. However, the ceilometer recorded a higher MLH at approximately 1600 m, where there was a sudden change in the backscatter gradient. When we measured the $PM_{2.5}/PM_{10}$ ratio at this moment, we found that the ratio was only 0.15, a clear characteristic of a sand-dust crossing. Due to the large number of dust particles, the aerosol concentrations became uniform below 1600 m. This led to a sudden change in the backscattering gradient at 1600 m and made it difficult to identify the real MLH at 1100 m; thus, an erroneously high MLH was determined. This result shows that sand-dust crossing is the main reason for the overestimations (Figs. 2 and 5).

Question 35
• (28258,26):
What is the "variation rate"?
Response 35
Thank you for your suggestion. We have deleted “the variation rate”.

Question 36
• (28258,28):
It is not clear to which data points in Fig.2 the PM2.5/PM10 labels belong to. This must be clear, maybe by giving only the numbers without "PM2.5/PM10".
Response 36
Thank you for your suggestion. We have fixed it in Figure 2.

Question 37
• (28259,5ff):
Do I understand correctly what has been done? The authors identify cases, where the MLH from the ceilometer strongly differs from the radio sounding (under- and overestimates). These cases (and as a consequence specific meteorological conditions as e.g. cold air masses and dust occurrence) are excluded from the further investigation. An alternative approach would have been to try to correct the MLH from the ceilometer to consider an unbiased data set of meteorological situations. I

recommend to revise the whole paragraph to make absolutely clear what have been done.

Response 37

Thank you for your suggestion. You are right. We have revised this paragraph as follows.

For underestimations, the meteorological data were used to eliminate the periods when cold air passed with a sudden change in temperature and WS. For overestimations, we referred to the sand-dust weather almanac to identify the sand-dust days (CMA, 2012, 2013, 2014, 2015). If there was no sand-dust crossing, the ratio of $PM_{2.5}$ to PM_{10} might almost exceed 50% (Liu et al., 2014). A sudden decrease in the ratio to 30% or lower usually indicates a sand-dust crossing. Using this principal, the exact times of sand-dust starting and ending were determined as the times at which the ratio of $PM_{2.5}$ to PM_{10} suddenly decreased or increased, respectively. Finally, the data obtained during the sand-dust periods were eliminated. After the screening process, the post-elimination ceilometer data and meteorological radiosondes are strongly correlated, with a correlation coefficient greater than 0.9, demonstrating the effectiveness of the elimination method (Fig. 6). Consequently, the elimination results are good. This method replaces the time-consuming method of filtering the data manually and is of great practical value for future measurements of MLH with ceilometers.

Question 38

• (28259,10):

"sand-dust weather almanac": What is this?

Response 38

The sand-dust weather almanac is like a statistic yearbook published every year. The main contents are the records of the sand-dust, which includes the time period, area and intensity of the sand-dust. In order to clarify this problem, we added the references in the revised manuscript.

Question 39

• (28259,15):

delete "and manipulability" (I don’t know, what is meant)

Response 39

Thank you for your suggestion. We have fixed it.

Question 40

• (28259,22):

What is meant by "high-quality..."?

Response 40

Because of the problems of the communication between CL31 and the data receiver, the data of CL31 was always interrupted during July to October 2009. The data from December 2009 to November 2012 were continuously observed. Therefore, the data

during this period were selected to do the analysis.

Question 41
• (28259,24 and 26):
"effectiveness of the data" → "availability..."
Response 41
Thank you for your suggestion. We have fixed it.

Question 42
• (28259,26 – 28260,5):
Are these correlations an independent result or a consequence of the filtering process described in the previous section?
Response 42
The results were a consequence of the filtering process described in the previous section.

Question 43
• (28260,8):
"The monthly average maximum for the daily minimum MLH": is this the "maximum of the monthly average of the daily minimum"?
Response 43
Thank you for your suggestion. We have fixed it.

Question 44
• (28260,16):
What are "platform periods"?
Response 44
Thank you for your suggestion. We have added some explanations about the platform and transition periods as follows.
As shown in Fig. 7b, two platform periods (from March to August and from October to January) and two transitional periods (February and September) occur for the monthly average MLH. The MLH is similar from October to January at approximately 500 m, and it is similar from March to August at approximately 700 m. February and September are the two transitional months and have values of approximately 600 m.

Question 45
• (28260,17):
Here, MLH are rounded and numbers like 600 m, 700 m are given. This does not fit to numbers like 351 m given previously; later (28264) heights are even given with one decimal place (this is nonsense with respect to any meteorological application). Please give all numbers in a consistent way. It would be worthwhile to add the variability of each height (each number is an average over almost 100 values [3 years, 31 days]).

What about the inter-annual change of the monthly means?
Response 45
Thank you for your suggestion. We are sorry for the misunderstandings. The numbers like 600 and 700m are not exact numbers like the other numbers. We just want to show the reader the MLH are consistent from March to August. In order to eliminate the misunderstanding, we have added “approximately” before these numbers.
Thank you for your suggestion about the variability of each MLH. We have added the variability in the revised manuscript.
From the figure as follows, you can see the inter-annual change of the monthly mean. It is very similar in different years, and no inter-annual trend can be found. Therefore, we used the averaged seasonal variation to do the analysis.

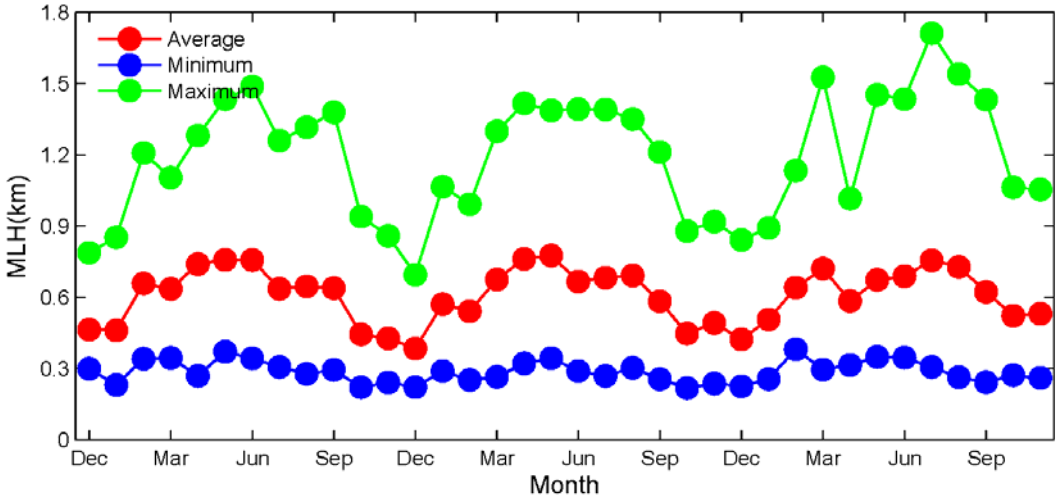

Figure S2 Monthly variations of MLH from December 2009 to November 2012 in Beijing.

Question 46
• (28260,26):
The "total radiation flux" should be defined: is total referring to the spectral range?
Response 46
Thank you for your suggestion. The total radiation flux was observed by CM11 (Kipp & zonen, Delft, Netherlands). The spectral range was 285-2800nm. We have added some description in the methodology section about this.

Question 47
• (28260,29):
"has determined seasonal variations in the MLH, because more data were eliminated for winter and spring,..."'. If this is true, the evaluation is somewhat questionable because the results should not depend on the sampling but on meteorological conditions. Please comment on this.
Question 48
• (28261,2):
"... winter and spring seasons are likely underestimated." This conclusion should be

explained in a convincing way.

Question 49

• (28261,3):

"To avoid the influence of data elimination on the study, ...". This is certainly a good idea (see comment on 28260,29), but it is not clear how the determination of the correlation with the sensible heat helps. By the way: if the sensible heat is determined at several heights, it should be clarified here, which heights are meant.

Response 47, 48 and 49

I am sorry for the misunderstanding. We have revised this paragraph as follows.

Other researchers have suggested that the seasonal variation in MLH may be related to radiation flux (Kamp and McKendry, 2010; Munoz and Undurraga, 2010), but our study was entirely consistent. As shown in Fig. 7b, although spring had a significantly higher total radiation flux than summer, the MLH in spring is equal to that in summer. This is because more data were eliminated for winter and spring, especially for weather with dry wind and relatively high MLH. Thus, using the monthly mean of MLH is not a good method by which to analyse the reasons for MLH variations.

To gain a better understanding of the reasons for the MLH variations, we use the daily mean instead of the monthly mean to do the analysis. As the simple framework in which we can analyse the MLH variations in Beijing, we consider the thermodynamic model of the mixing layer growth (Stull, 1988), as follows:

$$\frac{\partial z_i}{\partial t} = \frac{\overline{w'\theta_s'} - \overline{w'\theta_{z_i}'}}{\gamma z_i} \qquad (6)$$

where z_i is the MLH (m), t is the time (s), θ_s is the virtual potential temperature near the ground (K), θ_z is the virtual potential temperature in the top of the mixing layer (K), and γ is the lapse rate of the virtual potential temperature (K m^{-1}). Suppose the heat from the ground is the only way to warm the mixing layer and the heat flux at height z_i is zero, then the MLH is related to $\overline{w'\theta_s'}$. Considering that Q_H is defined as equation (1), MLH is correspondingly related to Q_H. Therefore, the relationship between daily changes in the Q_H at 280 m and MLH was analysed. The results showed that the average Q_H and MLH from 12:00 to 17:00 LT were well correlated, with a correlation coefficient of 0.65. Because net radiation (Q*) should be balanced by the Q_H, Q_E, and soil heat flux (Q_G) given as follows (Stull, 1988):

$$Q^* = Q_H + Q_{HE} + Q_G \qquad (7)$$

the strong correlation between the Q_H and MLH proves the dominant role of radiation in the variation of MLH (Fig.~8). This proves the dominant role of radiation in variation of MLH (Fig. 8).

Question 50

• (28261,16)

Why are only spring and summer discussed. What about the other seasons?

Response 50

The daily MLH range is 728, 828, 562, and 407m for spring, summer, autumn and

winter, respectively. The relatively low ranges in autumn and winter have obvious relationship with the low radiation flux. But it should be noted that summer has the lower radiation with a larger daily range than spring. Therefore, our study will emphasize on the reasons for the differences of the daily MLH ranges in summer and spring. By the way, we added the diurnal variations of winter and autumn in the supplement materials.

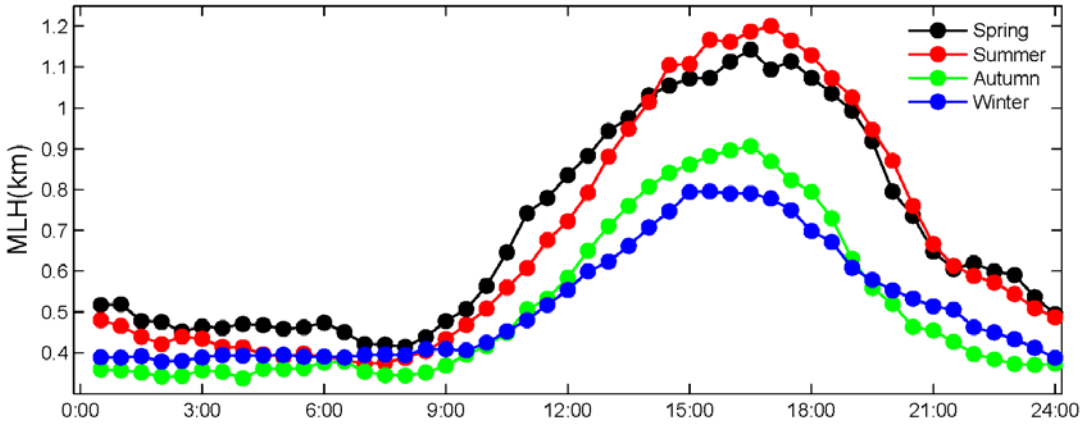

Figure 2 Diurnal variations of MLH in different seasons in Beijing

Question 51

• (28261,21)

"..only reaches 102 m/h..": is the difference to 114 m/h really significant? It seems to be within the error margins. Please discuss briefly.

Response 51

Thank you for your suggestion. The daily MLH range is 728, 828, 562, and 407m for spring, summer, autumn and winter, respectively. It is a significant difference between spring and summer for the daily range. After calculating the growth rate of MLH for each day, we do the T tests between the growth rate in spring and summer and find that the differences in the growth rates are significant ($P<0.05$).

Question 52

• (28261,22)

Here, the findings are discussed in terms of time (hours), previously four stages are introduced. It seems to be more consistent to use these terms here again.

Response 52

Thank you for your suggestion. Although the four stages are the same with that introduced before, the mountain-valley winds intersect the fast development stage into two parts. From 9:00 to 12:00 LT, the mountainous winds dominate Beijing, while the valley winds dominate Beijing after 12:00 LT. In order to interpret the influence of the mountain-plain winds, more precise stages should be pull-in.

Question 53

• (28261, 24):

"...convex variation characteristics...": there should be a better description, the present

text is not clear.

Question 54

• (28263, 5–6):

".. the air space from near surface to 300 m...": should be re-phrased, maybe just "troposphere below 300 m".

Question 55

• (28263, 18):

"...concave-down curvature...": there should be a better description.

Response 53, 54 and 55

Thank you for your suggestion. As shown in Fig. 9c, the mountainous winds are emerged at 02:00 LT during night near the ground, and then the influence of mountainous winds extend in the vertical direction. At 08:00 LT, troposphere below 300m is dominated by the mountainous winds.

In order to make this section clearer, we revised this section thoroughly as follows.

Although the daily average MLH is similar in spring and summer, the diurnal cycle exhibits obvious differences (Fig. 9a). At night-time in spring, the MLH is high and almost constant, whereas at night-time in summer, the MLH shows a gradual decreasing trend. After sunrise and before 12:00 LT, the rate of increase in the MLH is relatively high in spring, reaching 114 m/h, whereas the rate in summer is relatively low, 102 m/h. Between 12:00 and 14:00 LT in spring, the rate of increase in the MLH is 119 m/h, whereas in summer the rate of increase is significantly enhanced, reaching 165 m/h. These changes reflect the convex and concave characteristics during the development stage of the MLH in spring and summer, respectively.

According to the description in Sect. 3.2, variations in the MLH should exhibit a good linear relationship with the amount of radiation. Thus, the higher daily MLH range with lower radiation in summer is difficult to explain, suggesting that there are other reasons for this phenomenon. The development of MLH is mainly related to the turbulent energy and the production of the turbulent energy is closely related to two components: the heat flux caused by radiation ($\frac{g}{\overline{\theta_v}}\overline{w'\theta_v'}$) and the momentum flux generated by wind shear ($-\overline{u'w'}\frac{\partial \overline{u}}{\partial z}$) (Stull, 1988). Because the seasonal variation in heat flux is difficult to explain according to the aforementioned criteria, we analysed the seasonal variations of the horizontal wind vector.

To avoid the impact of near-surface buildings on the wind measurements, we selected the wind vector at 100 m on the Beijing tower. Figure 9b shows that there is obvious seasonal variation of the wind vector in Beijing. Winter is dominated by a northwest wind, and spring typically exhibits a northwest wind in the morning and a southwest wind in the afternoon. What matters most is the alternation between the mountainous winds that begin at 03:00 LT at night and the plain winds at 12:00 LT in the afternoon that begins to occur in summer. In September, the circulation of mountainous plain winds starts to weaken, and this circulation disappears in November.

Beijing is affected by the Siberian High in winter and spring; at these times, a strong prevailing northwest wind with dry air mass always occurs. However, the northward lift and westward intrusion of a subtropical high in summer causes the southern moist air mass with small WS to arrive and dominate. Because Beijing is located west of the Taihang Mountains and south of the Yanshan Mountains (Fig. 1), without the passage of large- or medium-scale meteorological systems in the summer, the local mountainous plain winds are superimposed on the southern air flow, and these two systems jointly affect the meteorological characteristics of the North China Plain.

With the surface cooling that occurs at night in summer, the cold air near the surface forms a shallow down-sliding flow from the northeast to the southwest; this is called the downslope wind or cold drainage flow. The cold air flows into the plain and accumulates in a cold pool, increasing the thickness of the inversion layer, and the thickness of the mixing layer gradually decreases. After sunrise, the radiation increases; the MLH increases rapidly under the impact of thermal buoyancy lift, and this type of cold drainage flow is maintained until 12:00 LT. After 12:00 LT, the plain wind from the southwest gradually dominates and is maintained until approximately 03:00 LT in the morning of the next day. According to Fig. 9c, from 03:00 LT to 12:00 LT in summer, the troposphere below 300 m gradually cools from low to high due to the cold drainage flow in the northeast direction, and the MLH exhibits a gradually decreasing trend from 03:00 to 06:00 LT. However, this trend does not occur in spring (Fig. 9a). Similarly, between 09:00 and 12:00 LT in summer, the cold drainage flow suppresses the development of the MLH with a low growth rate; in spring, without this inhibitory effect, the growth rate of the MLH is high. After 12:00 LT in summer, the southerly plain wind causes the growth rate to increase between 12:00 and 14:00 LT.

In summary, the mountainous wind in summer causes the mixing layer to decline gradually at night; this also suppresses the development of the mixing layer before noon, and the prevalence of plain winds after noon causes the mixing layer to increase rapidly. Therefore, compared to spring, the regional circulation in summer produces a concave-down variation in the rapid development stage of the MLH in summer.

Question 56

• (28265, Eq. 1):

Every symbol must be defined.

Response 56

Thank you for your suggestion. We have added other equations and add the explanations of each symbol in the revised manuscript.

Question 57

• (28264-28265):

All numbers listed here should be summarized in a table for the different visibility

classes. This table should also include the definition of the classes (name, v-range). Then, it would be much easier to follow the arguments of the authors because the text is better to read. As a consequence the whole text can be rephrased to be absolutely concise. Don't use MLH with decimal places! Check if there is no confusion between "slight haze" and "light haze".

Response 57

Thank you for your suggestion. We have summarized a table to make this section clear and concise. Slight haze is a condition better than light haze, the corresponding visibility are 5km≤Vis<10km and 3km≤Vis<5km for slight and light haze, respectively (CMA, 2010).

Table 2 Statistics of thermos/dynamic parameters according to different visibility

	Clear day Vis≥10km	Slight haze 5km≤Vis<10km	Light haze 3km≤Vis<5km	Medium haze 2km≤Vis<3km	Heavy haze Vis<2km
WS(m/s)	3.8	2.5	2.1	2.0	1.8
RH(%)	43.3	63.1	73.4	79.6	86.4
MLH(m)	664	671	586	430	320
$Q^*(W/m^2)$	77.6	74.6	63.9	53.6	32.8
$Q_E(W/m^2)$	18.7	19.9	21.5	18.8	19.8
$Q_H(W/m^2)$	20.4	19.7	15.2	12.8	7.8
$\bar{e}(m^2/s^2)$	0.99	0.64	0.56	0.52	0.46
$u_*(m/s)$	0.45	0.32	0.28	0.26	0.23
$BT(m^2/s^3)$	0.67	0.64	0.49	0.39	0.24
$ST(m^2/s^3)$	1.02	0.66	0.37	0.26	0.23

WS: wind speed; RH: relative humidity; Q*: net radiation; Q_E: latent heat; Q_H: sensible heat; $\bar{e}$: TKE per unit mass; u_*: friction velocity; BT: buoyancy term of the TKE; ST: shear term of the TKE.

We have also rewritten this paragraph as follows.

To analyse variations in the thermal dynamic parameters inside atmospheric mixing layers under different degrees of pollution, visibility was used as a reference. WS, RH, Q_H, Q_E, u_*, and TKE at 280 m were obtained under different visibility conditions (Tab. 2 and Fig. 10). Clear days were defined as days when the visibility is ≥10 km, and slight, light, medium, and heavy haze pollution corresponded with 5 km≤visibility<10 km, 3≤visibility<5 km, 2 km≤visibility<3 km and visibility<2 km, respectively (CMA, 2010). On clear days with atmospheric visibility ≥10 km, RH was the lowest, with an average of 43.3%, and Q_H, u_* and TKE were the highest, averaging 20.4 W m^{-2}, 0.45 m s^{-1}, and 0.99 m^2 s^{-2}, respectively. The MLH was 664 m on average, and the maximum in the afternoon reached 1145 m. Compared with clear days, during light haze pollution the RH significantly increased to 63.1%, and the u_* and TKE significantly declined to 0.32 m s^{-1} and 0.64 m^2 s^{-2}, respectively, with a reduction of approximately 30%; the Q_H and MLH were 19.7 W m^{-2} and 671 m, respectively, without any significant changes. With the pollution aggravated, the RH continued to increase; during light, medium, and heavy haze it reached 73.4,

79.6, and 86.4%, respectively. The u_* and the TKE remained almost constant, and the Q_H and the MLH showed a declining trend. The measured values under light, medium, and heavy haze were as follows: u_* was 0.28, 0.26, and 0.23 m s^{-1}, respectively; TKE was 0.56, 0.52, and 0.46 m^2 s^{-2}, respectively; Q_H was 15.2, 12.8, and 7.8 W m^{-2}, respectively; and the MLH was 586, 430, and 320 m, respectively.

Question 58
• (28266, 25):
"...exhibit a conflicted state." That is meant?
Response 58
Thank you for your suggestion. We have revised it as follows.
However, although the atmospheric diffusion capability is much better in spring and summer and the VC in summer can be 1.7 times higher than in autumn and winter, the visibility is lowest (~9 km) and the PM2.5 concentration is highest (~85 μg m^{-3}) in summer (Fig. 12a). By focusing on visibility≥10 km and visibility<10 km separately, we find that the frequency of haze occurrence is highest (up to 73%) in summer, whereas it is approximately 40% in other seasons (Fig. 12b). Therefore, strong diffusion capability cannot explain the occurrence of heavy pollution in summer.

Question 59
• (28267, 17):
"Previous studies..." Give citations!
Response 59
Thank you for your suggestion. We have fixed it.

Question 60
• (28268, 14):
"...and the critical threshold is 80 %." Where is this statement coming from? Is it a definition/estimate of the authors?
Response 60
I am sorry for the misunderstanding. We do the analysis of the correlation between MLH and visibility and find the correlation shows a sudden change when the RH is beyond 80% (Table S1), so 80% is used as the threshold for the RH. In order to clarify this question, we have rewritten this paragraph as follows.
Table S1 Correlation coefficients (R) between the MLH and visibility according to different RH

	RH≤40	40<RH≤50	50<RH≤60	60<RH≤70	70<RH≤80	80<RH≤90	RH>90
R	0.15	0.04	0.01	0.09	0.41	0.70	0.77

Question 61
• (28268, 17):
"We found that the..." I don’t understand this and the next sentence? Is the order of visibilities and names (10 km does not correspond to heavy haze) correct?
Please clarify!
Response 61
Thank you for your suggestion. We have added a table according to your suggestion in question 57. In that table, the different degrees of air pollution are clarified in detail. In addition, the sequence of the degrees of air pollution is not the same with the context, which may induce the reader misunderstanding. Therefore, we revised this paragraph. Please see response 60.

Question 62
• (28269, 16):
"exhibits the feature": please re-phrase
Response 62
Thank you for your suggestion. We have fixed it.

Question 63
• (28269, 17):
"variation in the MLH": please re-phrase
Response 63
Thank you for your suggestion. We have fixed it.

Question 64
• (28270, 1):
"slight haze": should be light haze?
Response 64
Thank you for your suggestion. We have clarified the degrees of the haze, please see the response 57.

Question 65
• Fig. 1
A scale would be helpful
Response 65
Thank you for your suggestion. We have revised the map as follows.

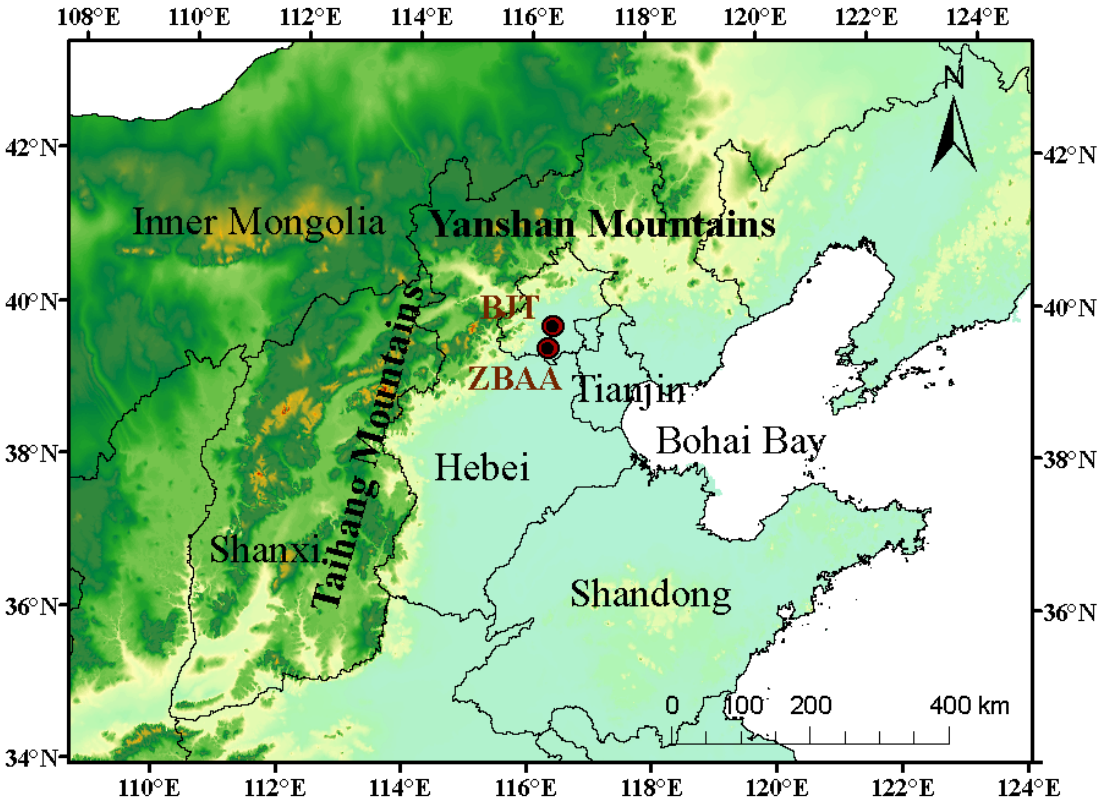

Question 66
• Fig. 10
"visibility levels": levels can be omitted.
Response 66
Thank you for your suggestion. We have fixed it.

Question 67
• all Figs.
whenever possible include a x/y-grid
Response 67
Thank you for your suggestion. We have added the grid in Figs. 2, 3, 4, 6, 8 and 11.

References
China Meteorological Administration (CMA). Observation and forecasting levels of haze. QX/T 113-2010, Beijing, 2010.
China Meteorological Administration (CMA): sand-dust weather almanac (2009), China Meteorological Press, Beijing, 2012.
China Meteorological Administration (CMA): sand-dust weather almanac (2010), China Meteorological Press, Beijing, 2013.
China Meteorological Administration (CMA): sand-dust weather almanac (2011), China Meteorological Press, Beijing, 2014.
China Meteorological Administration (CMA): sand-dust weather almanac (2012), China Meteorological Press, Beijing, 2015.

Ding, G. A., Chen, Z. Y., Gao, Z. Q., Yao, W. Q., Li, Y., Cheng, X. H., Meng, Z. Y., Yu, H. Q., Wong, K. H., Wang, S. F., and Miao, Q. J.,2005. Vertical structures of PM10 and PM2:5 and their dynamical character in low atmosphere in Beijing urban areas, Sci. China Ser. D-Earth Sci., 35, 31-44.

Eresmaa, N., Karppinen, A., Joffre, S. M., Räsänen, J., and Talvitie, H.: Mixing height determination by ceilometer, Atmos. Chem. Phys., 6, 1485-1493, doi:10.5194/acp-6-1485-2006, 2006.

Hu, B., Wang, Y. S. and Liu, G. R.: Relationship between net radiation and broadband solar radiation in the Tibetan Plateau. Adv. Atmos. Sci., 29(1), 135-143, doi: 10.1007/s00376-011-0221-6, 2012.

Liu, Z, Hu, B., Wang, L., Wu, F., Gao, W., and Wang, Y.: Seasonal and diurnal variation in particulate matter (PM10 and PM2.5) at an urban site of Beijing: analyses from a 9-year study, Environ. Sci. Pollut. R., 22, 627-642, 2015.

Muñoz Ricardo C. and Undurraga Angella A., 2010: Daytime Mixed Layer over the Santiago Basin: Description of Two Years of Observations with a Lidar Ceilometer. J. Appl. Meteor. Climatol., 49, 1728–1741.

Seibert Petra, Beyrich Frank, Gryning Sven-Erik, Joffre Sylvain, Rasmussen Alix, Tercier Philippe, Review and intercomparison of operational methods for the determination of the mixing height, Atmos. Environ., 34(7), 2000, 1001-1027.

Song Tao, Wang Yuesi, Carbon dioxide fluxes from an urban area in Beijing, Atmospheric Research, 106, 2012, 139-149, http://dx.doi.org/10.1016/j.atmosres.2011.12.001.

Stull, R.B., 1988. An Introduction to Boundary Layer Meteorology. Kluwer Academic Publishers, Dordrecht, 665 pp.

Wiegner, M.,Madonna, F, Binietoglou, I., Forkel, R., Gasteiger, J., Geiß, A., Pappalardo, G., Schäfer, K., and Thomas, W.: What is the benefit of ceilometers for aerosol remote sensing? An answer from EARLINET, Atmos. Meas. Tech., 7, 1979–1997, doi:10.5194/amt-7-1979-2014, 2014.

Zhang Qiang, Quan Jiannong, Tie Xuexi, Li Xia, Liu Quan, Gao Yang, Zhao Delong, Effects of meteorology and secondary particle formation on visibility during heavy haze events in Beijing, China, Sci of The Total Environ., 502(1), 2015, 578-584, http://dx.doi.org/10.1016/j.scitotenv.2014.09.079.

Response to comments by referee 2

We would like to thank you for your comments and helpful suggestions. We revised our manuscript according to these comments and suggestions.

General comments:
Visibility was used as a proxy for pollution, why not directly PM concentrations ?
The paper is occasionally very hard/heavy to read: page 28264 is a perfect example of the general problem : whole page is filled with lists of numbers and extremely long sentences without any clear structuring, so at the end the reader is definitely losing the whole idea of the text, and it is very hard to see what all those.
Responses：
Thank you for your kindly comments and suggestions.
In order to characterize the degree of the air pollution in Beijing, PM concentration was a good indicator. However, haze is defined by the visibility in China as shown in Table 2 in the revised manuscript (CMA, 2010), and it was remarkably negative correlated with PM concentration (Yang et al., 2015). Considering the occasionally missing data of the PM, visibility was used as an index to classify the air pollution degree.
We are sorry for the bad presentation in our manuscript. In the revised version of our manuscript, several long paragraphs were separated into some small parts or rephrased concisely. Afterwards, a native speaker revised our manuscript to make the language better understanding for the reader.

Specific comments：
Question 1
(25254):
While with most other numbers (like mixing height with 10 cm accuracy?) there are obviously too many decimals given in the paper - with this for some strange reason far to few; 1km accuracy is not normally very acceptable with a station location?
Response 1
Thank you for your suggestions. We have revised the significant digits thoroughly according to your suggestions.

Question 2
(28255):
We defined all of the meteorological sounding profiles as a convection state when they exhibited negative lapse rates for the virtual potential temperature within 200 m and bulk Richardson number within 100 m, and the other profiles were defined as a stable state."
Would it not be useful to consider/define also neutral cases? (See also comment below)
Question 3
• (28258):

“Therefore, the near-neutral atmospheric stratification that occurs when a cold air mass passes through is the main cause for the serious underestimation in the observation results by the ceilometer.”
This seems to be a logical conclusion: however, it remains still unclear, was it really verified that these situations were truly neutral? The paper only states that these situations were corresponding to “conditions with low relative humidity and large wind speed, with winds mostly from the north” – but no direct proof on the “neutrality” is given?
Response 2 and 3
Thank you for your suggestions. The neutral condition seldom emerged in the actual environment. However, the mixing layer is near-neutral during strong winds and cloudy day. In our analyses, the overestimations are emerged during strong winds crossing, not all the near-neutral conditions. Otherwise, in the process of the analyses, we found it was very difficult to define the neutral condition because of the influence of the urban canopy, which affected the lapse rate of the virtual potential temperature. Therefore, we used two meteorological conditions as same as the former studies (Eresmaa et al., 2006; Münkel et al., 2007). Although we just used two meteorological conditions, we showed the evidence of the bulk Richardson number is approximately 0 for the near-neutral condition (Fig. S1).

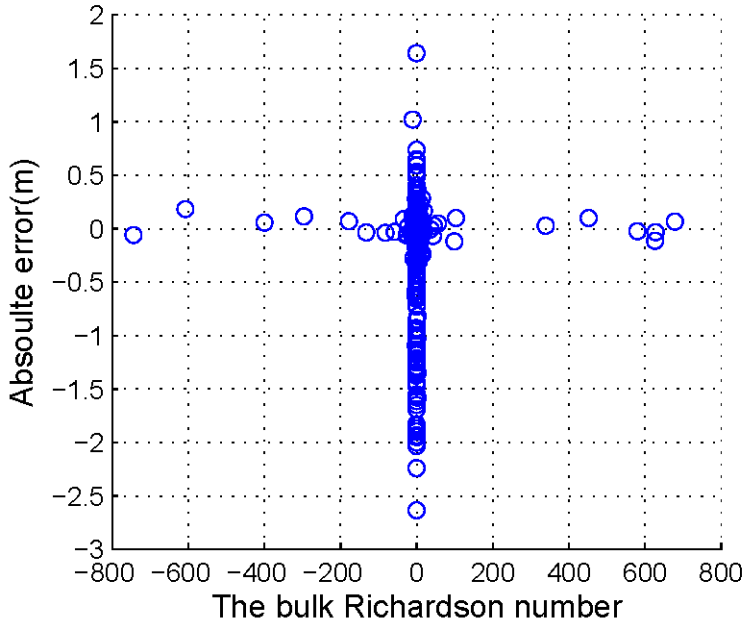

Figure S1 Relationship between the bulk Richardson number and the absolute error of the measured MLH.

Question 4
(28259):
“After determining the reasons for the underestimations and overestimations in the ceilometer data, the results with large errors according to certain principles must be eliminated.”
Yes, that is an easy option – much better one would be to correct the mixing height

algorithm so, that it would give better estimates in these conditions- was this approach doomed to be impossible?

Response 4

Thank you for your suggestions. Interpreting data from aerosol lidars is often not straightforward, because the detected aerosol layers are not always the result of ongoing vertical mixing, but may originate from advective transport or past accumulation processes (Russell et al., 1974; Coulter, 1979; Baxter, 1991; Batchvarova et al., 1999). Therefore, improving the algorithm cannot solve the underestimations and overestimations of the ceilometer observations, and the only option to correct the MLH is to eliminate the data with large AE. After determining the reasons for the underestimations and overestimations of the ceilometer results, the elimination is much easier to implement.

Question 5

• (28259):

"The elimination results are good, and this method replaces the time consuming method of filtering the data manually, which is of great practical value for future measurements of MLH with ceilometers. For overestimations, we used the date of dust occurrence based on the sand–dust weather almanac to eliminate the time periods of dust crossing when the ratio of PM2.5 and PM10 suddenly decreases.

Now, it would be extremely important to document what was exactly done here- was the PM-ratio used at all, or just some undocumented "sand-dust weather almanac"??

This method itself seems to be one of the very useful/new things developed, but unfortunately it remains very unclear how this could be utilized in e.g. other locations?

Response 5

Thank you for your suggestion. The sand-dust weather almanac is like a yearbook of sand-dust, which is compiled by the China Meteorological Administration. In order to make this paragraph clearer, we added some description in the methodology section and rewrote this paragraph as follows.

The methodology section:

To identify the sand-dust crossing, the ratio of $PM_{2.5}$ and PM_{10} was used as an index. If there was no sand-dust crossing, the ratio of $PM_{2.5}$ to PM_{10} might almost exceed 50% (Liu et al., 2014). A sudden decrease in the ratio to 30 % or lower and PM_{10} concentration higher than 500 μg m^{-3} usually indicate a sand-dust crossing. The ground observations of $PM_{2.5}$ and PM_{10} during the same period were made by the ambient particulate monitor (RP1400a, Thermo Fisher Scientific, USA). The data were acquired at a time resolution of 5 min and processed with a resolution of 60 min. A detailed description is provided by Liu et al. (2014).

Section 3.1:

For underestimations, the meteorological data were used to eliminate the periods when cold air passed with a sudden change in temperature and WS. For overestimations, we referred to the sand-dust weather almanac to identify the

sand-dust days (CMA, 2012, 2013, 2014, 2015). Using the principal described in Sect.2.1.1, the exact times of sand-dust starting and ending were determined as the times at which the ratio of $PM_{2.5}$ to PM_{10} suddenly decreased or increased, respectively. Finally, the data obtained during the sand-dust periods were eliminated.

Question 6
(28259):
"First, the effectiveness of the data must be verified after performing the elimination by the aforementioned method. The results of the evaluation indicate that the effectiveness of the data in different seasons is significantly negatively correlated with wind speed and significantly positively correlated with relative humidity"
"Effectiveness" probably not the best possible label for availability of useful MLH data. The Figure 7 indicates that the above statements may be true, but the text "explaining" the reasons for over– and underestimation fails to give a clear explanation why this is to be expected: the text should be restructured so that the reasons behind Fig.7 would come more clear.
Response 6
Thank you for your suggestion. We have revised the "effectiveness" to "availability". In addition, we also have rephrased this paragraph to make the explanation clearer as follows.
To provide a detailed description of variations in the MLH, we selected continuous measured MLH and meteorological data over a 3-year period (from December 2009 to November 2012). First, the availability was verified after the MLH elimination. The results of the evaluation indicate that the availability in different seasons is significantly negatively correlated with WS and positively correlated with RH (Fig. 7a). For spring and winter seasons with large WS and low RH, the availability is low, whereas for summer and autumn seasons with small WS and high RH, the availability is high. In particular, the availability is lowest in January at 63.5% and highest in June at 95.0%. The successful retrieval of MLH over the 3-year period is approximately 80%, much higher than in a previous study (Munoz and Undurraga, 2010).

Question 7
• (28261):
"To avoid the influence of data elimination on the study, we analysed the relationship between daily changes of the mixing layer and the sensible heat flux and found that the average MLH from 12:00 to 17:00 LT and the sensible heat flux were well correlated (Fig. 8) and had a correlation coeffcient of 0.65, which characterizes the dominant role of radiation in the variations" ? Not really clear what the beginning of the sentence says : "avoid" ? ! radiation is NOT a synonym for sensible heat flux – this should be clear in the text +This would be a perfect place for on equation /reference to some well-known formulas connecting sensible heat flux & MH ? any references to well-known MH formulas!

Response 7

Thank you for your suggestions. We rewrote this paragraph and added the relationship between the sensible heat and MLH. The revised paragraph is as follows.

To gain a better understanding of the reasons for the MLH variations, we use the daily mean instead of the monthly mean to do the analysis. As the simple framework in which we can analyse the MLH variations in Beijing, we consider the thermodynamic model of the mixing layer growth (Stull, 1988), as follows:

$$\frac{\partial z_i}{\partial t} = \frac{\overline{w'\theta'_s} - \overline{w'\theta'_{z_i}}}{\gamma z_i} \qquad (6)$$

where z_i is the MLH (m), t is the time (s), θ_s is the virtual potential temperature near the ground (K), θ_z is the virtual potential temperature in the top of the mixing layer (K), and γ is the lapse rate of the virtual potential temperature (K m^{-1}). Suppose the heat from the ground is the only way to warm the mixing layer and the heat flux at height z_i is zero, then the MLH is related to $\overline{w'\theta'_s}$. Considering that Q_H is defined as equation (1), MLH is correspondingly related to Q_H. Therefore, the relationship between daily changes in the Q_H at 280 m and MLH was analysed. The results showed that the average Q_H and MLH from 12:00 to 17:00 LT were well correlated, with a correlation coefficient of 0.65. Because net radiation (Q*) should be balanced by the Q_H, Q_E, and soil heat flux (Q_G) given as follows (Stull, 1988):

$$Q^* = Q_H + Q_{HE} + Q_G \qquad (7)$$

the strong correlation between the Q_H and MLH proves the dominant role of radiation in the variation of MLH (Fig.~8). This proves the dominant role of radiation in variation of MLH (Fig. 8).

Question 8

(28262):

"Two components are closely related to turbulent energy: the heat flux caused by radiation and the momentum flux generated by wind shear" Why not simply state/show how (equation?) how these are EXACTLY related ?

Response 8

Thank you very much. We have added the equation in the revised manuscript.

Question 9

(28263):

"In summary, the mountainous wind in summer causes the mixing layer to gradually decline at night, which suppresses the development of the mixing layer before noon, and the prevalence of plain winds after noon causes the mixing layer to increase rapidly. Therefore, this regional circulation leads to the concave-down variation in the fast development stage of the mixing layer in summer compared to the spring. <- Ref Figure 9. Figure 9 does NOT really show significant differences between MLH spring vs summer? So the long discussion & strong statements seem to be not justified? Or is there a real reason why even those small differences are so significant/important?

Response 9

Thank you for your suggestions. I am very sorry for the misunderstanding because of language. In order to make this section clearer, we have rephrased this section and added some new analyses. The daily MLH range is 728, 828, 562 and 407 for spring, summer, autumn, and winter, respectively. It exhibits significant differences between spring and summer. If we do the T test for this two seasons, we find the differences in the growth rates are significant ($P<0.05$). Therefore, we revised this section as follows.

Question 10
(Fig10):
fraction velocity ->friction velocity
Response 10
Thank you for your suggestion. We have fixed it.

Question 11
• (28265):
Equation 1/the only equation in the paper.
If you present an equation you should explain all the terms, not just virtual(?) potential temperature Describing those all would probably soon also reveal that differentiating gravitational constant is not generally a good idea (<-error in at least in the buoyancy production and depletion term + dividing rho should be rho0..in the 3rd term ?)
Rersponse 11
Thank you for your suggestions. We have added the explanations of the other parameters in the equation and revised the equation as follows.
In order to verify these results, we examined the TKE budget equation. If we presume a horizontal average and neglect the advection of wind, then the forecast equation of the TKE can be written as follows (Garratt, 1992):

$$\frac{\partial \bar{e}}{\partial t} = -\overline{u'w'}\frac{\partial \bar{u}}{\partial z} + \frac{g}{\bar{\theta}_v}\overline{w'\theta_v'} - \frac{\partial(\overline{w'e})}{\partial z} - \frac{1}{\rho}\frac{\partial(\overline{w'p'})}{\partial z} - \varepsilon$$

where θv is the virtual potential temperature, g is the acceleration of gravity (m s^{-2}), ρ is the air density (kg m^{-3}), u is the horizontal velocity (m s^{-1}), w is the vertical velocity (m s^{-1}), p is the air pressure (Pa), z is the height (m), e is the TKE (m^2 s^{-2}), ε is the dissipation term of TKE (m^2 s^{-3}).
Question 12
• (28265):
"The turbulent transportation term does not generate or destroy the TKE, and it just moves the TKE from one position to another position or redistributes the TKE. This term remains constant at zero in the entire mixing layer" Well, the first sentence reasonably correct, but don't quite get the meaning of the second one? Sounds like you claim the second term to be zero everywhere?
Response 12
I am sorry for the misunderstanding. "This term remains constant at zero in the entire

mixing layer" have been revised to "the integral of this term in the mixing layer remains constant at zero."

Question 13
(Conclusions):
More general on the conclusion "The presented results on the atmospheric mixing layer and its thermal dynamic structure under different degrees of pollution provide a scientific basis for improving the meteorological and atmospheric chemistry models and the forecasting and warning of atmospheric pollution."
My first impression is that "scientific bases" is not the correct term here-maybe more like "useful empirical information " or something similar: the paper does not really present any new parameterizations or models , not probably even directly supporting that.
Response 13
Thank you for your suggestion. We have fixed "scientific basis" to "useful empirical information".

References
Batchvarova, E., Cai, X., Gryning, S. E., Steyn, D.: Modelling internal boundary layer development in a region with complex coastline. Bound.-Lay. Meteorol., 90, 1-20, 1999.
Baxter, R. A.: Determination of mixing heights from data collected during the 1985 SCCCAMP field program. J. Appl. Meteorol., 30, 598-606, 1991.
China Meteorological Administration (CMA): Observation and forecasting levels of haze, QX/T 113-2010, Beijing, 2010.
China Meteorological Administration (CMA): Sand-dust weather almanac (2009), China Meteorological Press, Beijing, 2012.
China Meteorological Administration (CMA): Sand-dust weather almanac (2010), China Meteorological Press, Beijing, 2013.
China Meteorological Administration (CMA): Sand-dust weather almanac (2011), China Meteorological Press, Beijing, 2014.
China Meteorological Administration (CMA): Sand-dust weather almanac (2012), China Meteorological Press, Beijing, 2015.
Coulter, R. L.: A comparison of three methods for measuring mixing layer height. J. Appl. Meteorol., 18, 1495-1499, 1979.
Eresmaa, N., Karppinen, A., Joffre, S. M., Räsänen, J., and Talvitie, H.: Mixing height determination by ceilometer, Atmos. Chem. Phys., 6, 1485-1493, doi: 10.5194/acp-6-1485-2006, 2006.
Liu, Z, Hu, B., Wang, L., Wu, F., Gao, W., and Wang, Y.: Seasonal and diurnal variation in particulate matter (PM10 and PM2.5) at an urban site of Beijing: analyses from a 9-year study, Environ. Sci. Pollut. R., 22, 627-642, 2015.
Münkel, C., Eresmaa, N., Räsänen, J., and Karppinene, A.: Retrieval of mixing height and dust concentration with lidar ceilometer, Bound.-Lay. Meteorol., 124, 117--128, 2007.

Garratt, J.R., 1992. The Atmospheric Boundary Layer. Cambridge University Press, Cambridge, UK.
Muñoz Ricardo C. and Undurraga Angella A., 2010: Daytime Mixed Layer over the Santiago Basin: Description of Two Years of Observations with a Lidar Ceilometer. J. Appl. Meteor. Climatol., 49, 1728–1741.
Stull, R.B., 1988. An Introduction to Boundary Layer Meteorology. Kluwer Academic Publishers, Dordrecht, 665 pp.
Russell, P. B., Uthe, E. E., Ludwig, F. L., Shaw, N. A.: A comparison of atmospheric structure as observed with monostatic acoustic sounder and lidar techniques. J. Geophys. Res., 79, 5555-5566, 1974.
Yang, Y. R., Liu, X. G., Qu, Y., An, J. L., Jiang, R., Zhang, Y. H., Sun, Y. L., Wu, Z. J., Zhang, F., Xu, W. Q., and Ma, Q. X.: Characteristics and formation mechanism of continuous hazes in China: a case study during the autumn of 2014 in the North China Plain, Atmos. Chem. Phys., 15, 8165-8178, doi:10.5194/acp-15-8165-2015, 2015.